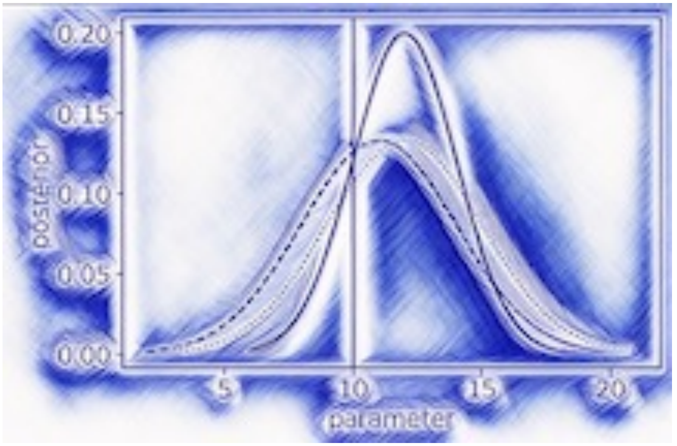

High-energy experimental imaging of nuclear shapes for precise constraints on QGP initial conditions

Chunjian Zhang

Fudan University

September 8, 2025, Wuhan

Precision Frontier of QCD Matter: Inference and Uncertainty Quantification

Outline

I. Nuclear structure across energy scales

II. Nuclear deformation in ^{238}U and ^{129}Xe nuclei

III. Nuclear deformation and neutron skin in ^{96}Ru and ^{96}Zr nuclei

IV. Nucleonic clustering in light ^{16}O nucleus

V. Conclusions and outlooks

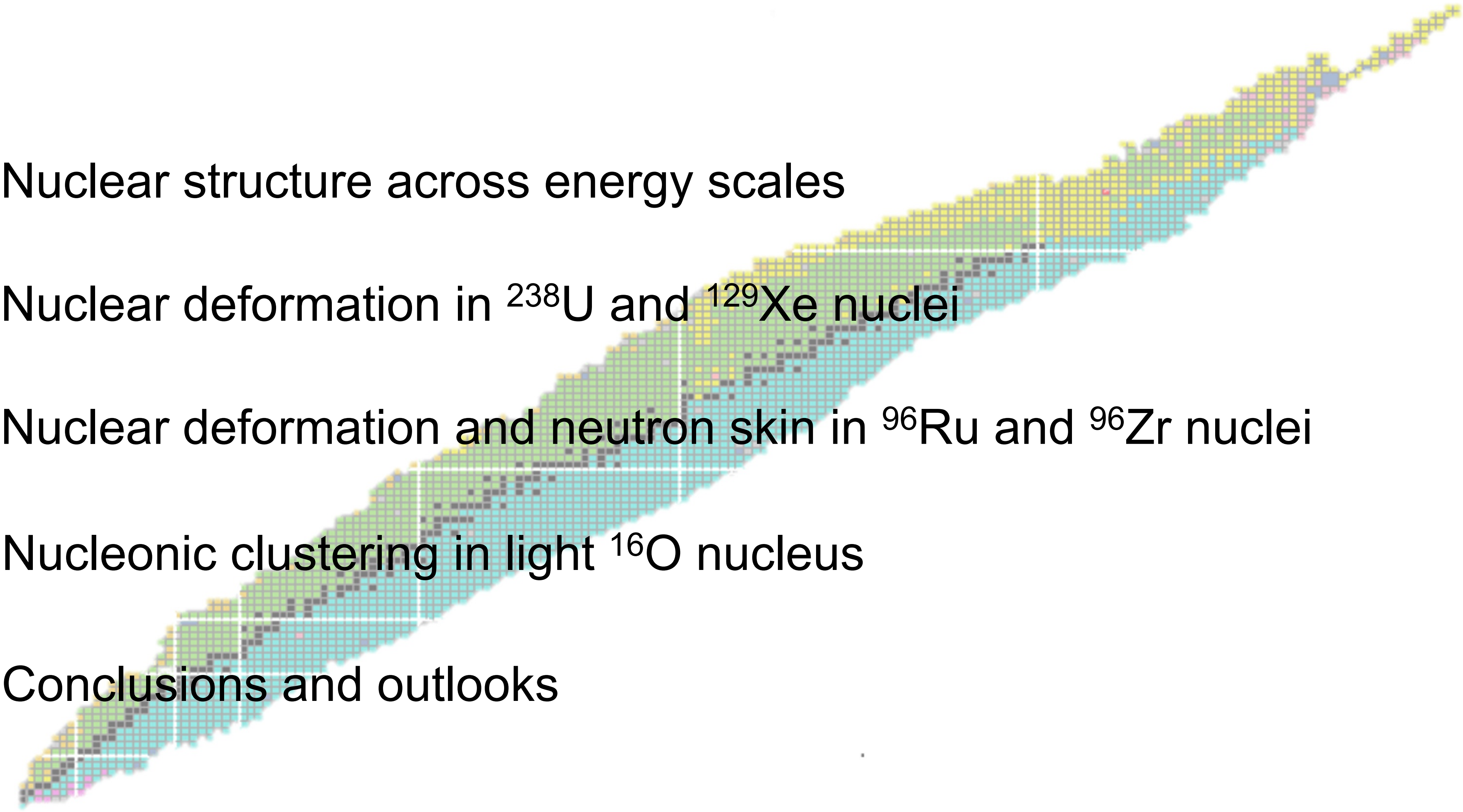

Shape of atomic nuclei

Emergent phenomena of the many-body quantum system, govern by short-range strong nuclear force

- Quadrupole/octupole/hexadecapole deformations
- Clustering, halo, skin, bubble…
- Non-monotonic evolution with *N* and *Z*

A. Andreyev et al., Nature 405, 430 (2000)
S. Cwiok et al.,Nature 433, 705 (2005)
LP Gaffney P. Butler et al., Nature 497, 199 (2013)
A. Trzcinska et al., PRL 87, 082501 (2001)
A. M. Centelles et al., PRL 102, 122502 (2009)
J.P. Ebran et al. Nature 487, 341 (2012)

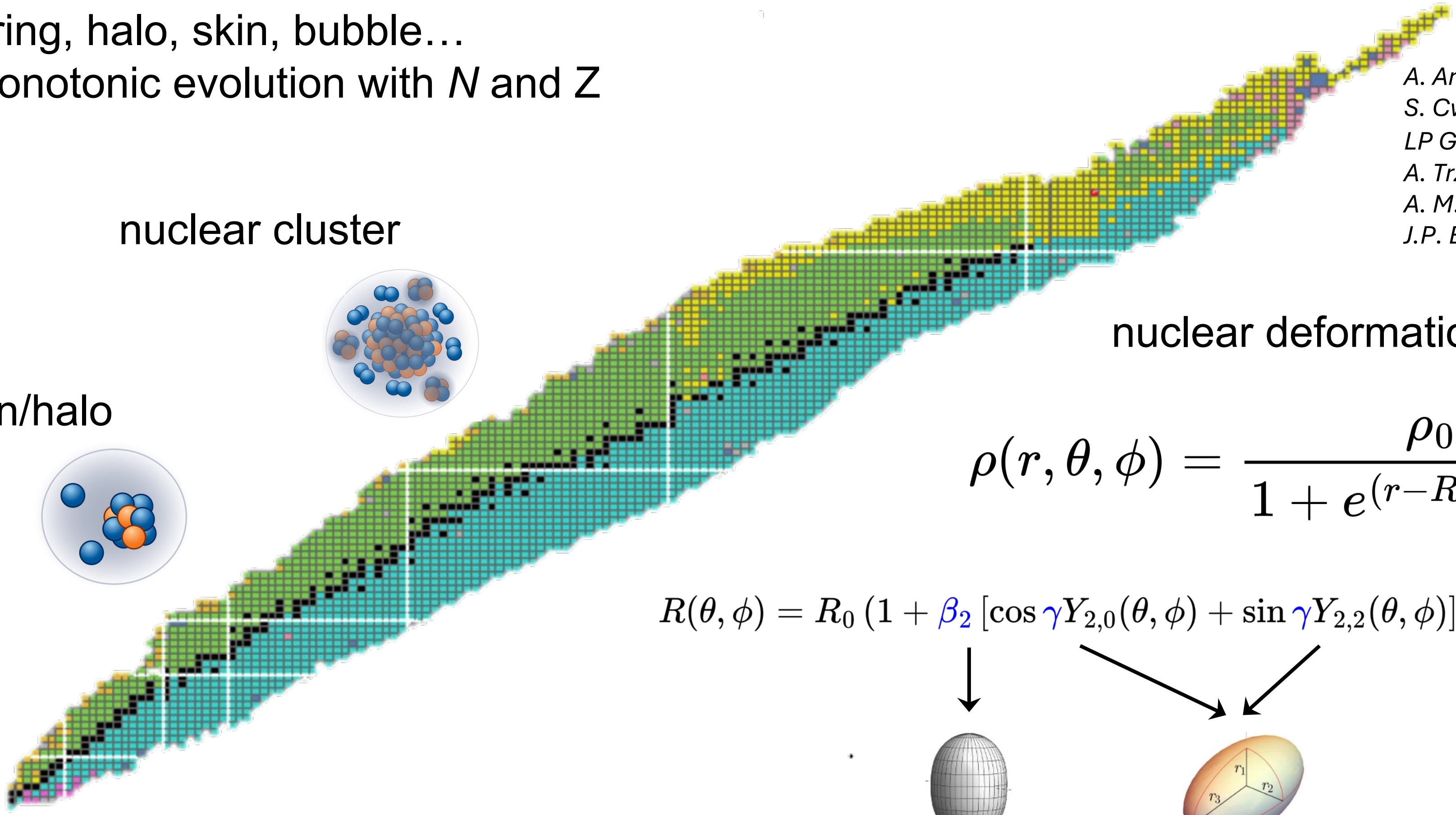

nuclear cluster

neutron skin/halo

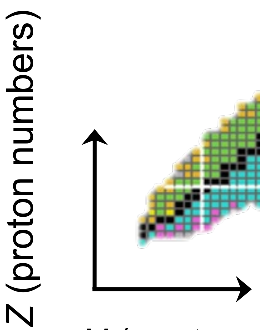

N (neutron numbers)

nuclear deformation

$$\rho(r,\theta,\phi) = \frac{\rho_0}{1+e^{(r-R(\theta,\phi))/a_0}}$$

$$R(\theta,\phi) = R_0\left(1+\beta_2\left[\cos\gamma Y_{2,0}(\theta,\phi)+\sin\gamma Y_{2,2}(\theta,\phi)\right]+\beta_3 Y_{3,0}(\theta,\phi)+\beta_4 Y_{4,0}(\theta,\phi)\right)$$

Very rich landscape of shapes and other structures

Y. Ye, X. Yang, H. Sakurai, B. Hu, Nature Review Physics, 7, 21-37 (2025); Y. Ma, S. Zhang, Handbook of Nuclear Physics (2022)

Nuclear shape at low energy: long exposure

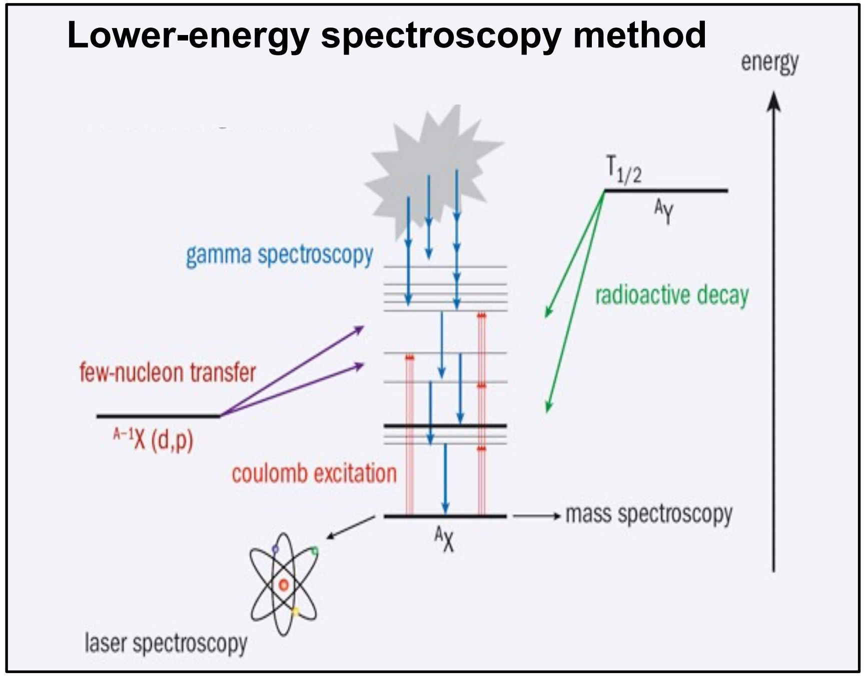

Traditional imaging method taken before destruction

→ Low energy spectroscopic methods probe a superposition of these fluctuations.
→ Instantaneous shapes not directly seen, but inferred from model comparison.

Each DOF has zero-point fluctuations within certain timescales.

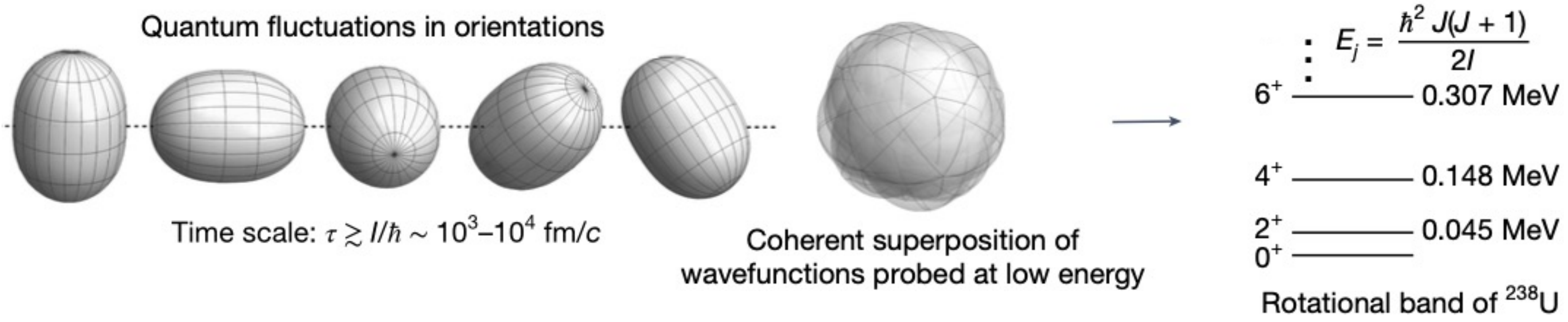

Nuclear shape at high-energy: short exposure

Emergent seeing shape directly require access to instantaneous nucleon distributions

$$\Psi\left(\mathbf{r}_1, \mathbf{r}_2 \ldots\right)$$

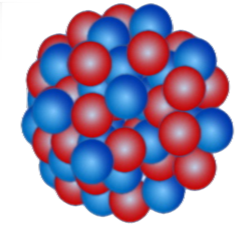

Will see all DOFs longer than exposure timescale: $\tau > \tau_{\mathrm{expo}}$

nucleons, hadrons, quark, gluons, gluon saturations

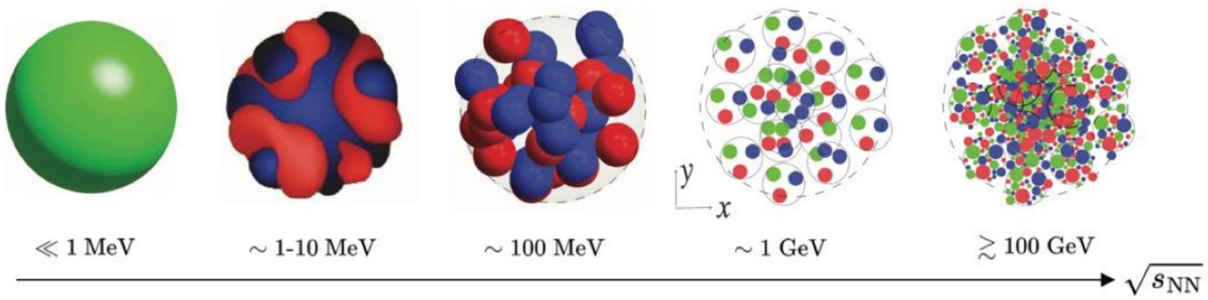

Hence concept of shape is collision energy dependent

$\epsilon_2 = 0$ $\qquad$ $\epsilon_2 \sim \frac{1}{\sqrt{A}}$

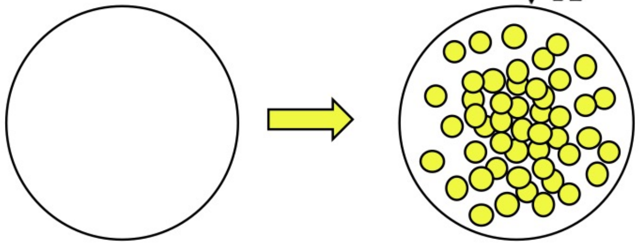

Spherical Woods-Saxon $\qquad$ Sampled with A nucleons

$$\boldsymbol{\epsilon}_2 = \underbrace{\boldsymbol{\epsilon}_0} + \underbrace{\boldsymbol{p}(\Omega)\beta_2} + \mathcal{O}\left(\beta_2^2\right)$$

$\sqrt{s}$-dependent quantum fluctuation induced shape

Global shape rotational vibrational

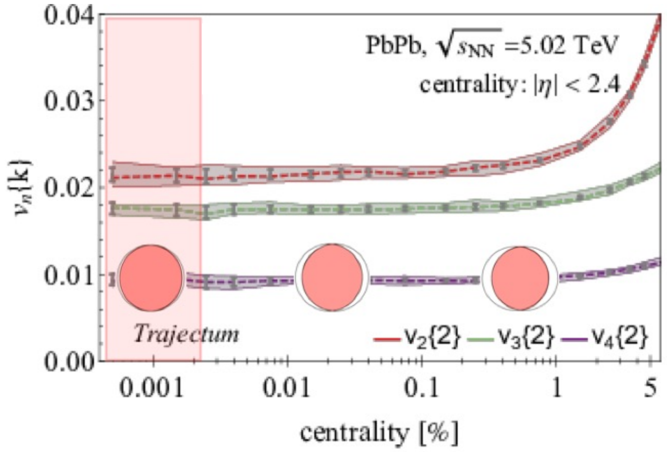

Imaging by smashing method

Take a snapshot | Evolution | Measurement

Nuclei collisions

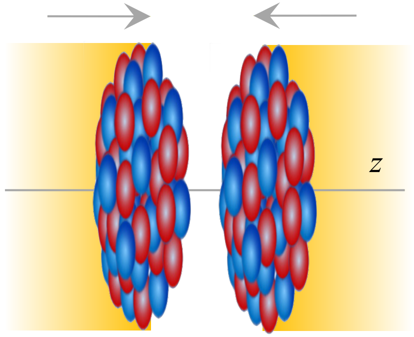

$T_{\mu\nu}(\tau = 0)$

$\tau \sim 2R_0/\Gamma \sim 0.1\text{fm}/c$
exposure

Pressure-driven expansion of Quark-gluon plasma (QGP) ⟶

$\partial_\mu T^{\mu\nu} = 0$, EOS, viscosity…

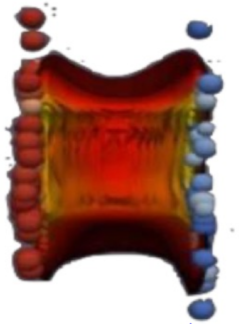

$\tau \sim 10\text{fm}/c$
expansion

free-streaming ⟶

$T_{\mu\nu}(\tau = \infty)$

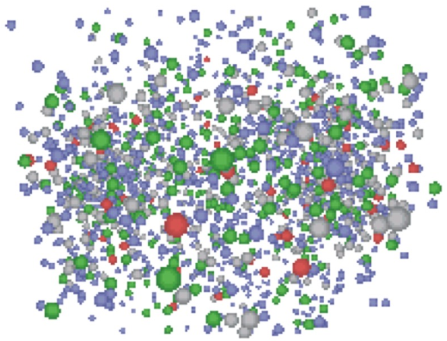

$\tau \sim 10^{15}\text{fm}/c$
detection

$T_{\mu\nu}(\tau = 0)$ snapshot ⟶ $\partial_\mu T^{\mu\nu} = 0$ evolution ⟶ $T_{\mu\nu}(\tau = \infty)$ measurement

J. Jia et al., Nucl. Sci. Tech 35, 220 (2024)

Image inferred after destruction

Imaging by smashing method

Take a snapshot | Evolution | Measurement

Nuclei collisions

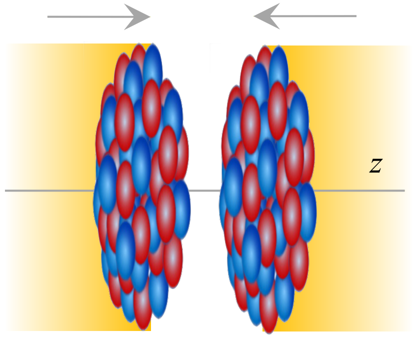

$T_{\mu\nu}(\tau = 0)$

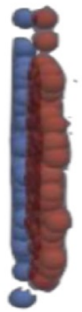

$\tau \sim 2R_0/\Gamma \sim 0.1\mathrm{fm}/c$
exposure

Pressure-driven expansion of Quark-gluon plasma (QGP)

$\partial_\mu T^{\mu\nu} = 0$, EOS, viscosity…

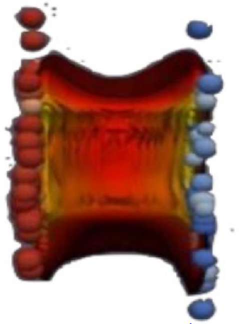

$\tau \sim 10\mathrm{fm}/c$
expansion

free-streaming

$T_{\mu\nu}(\tau = \infty)$

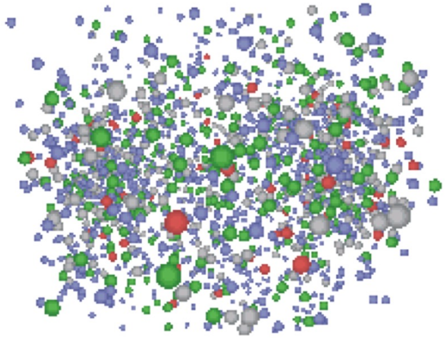

$\tau \sim 10^{15}\mathrm{fm}/c$
detection

Large entropy production enable a semi-classical description

- Initial condition is a fast snapshot of nuclear structure (<0.1fm/c)
- Transformed to the final state via hydrodynamic expansion
- Reverse-engineer to infer the snapshot, aided by large information output

J. Jia et al., Nucl. Sci. Tech 35, 220 (2024)

Ability to image ⟷ Understanding of the QGP

Imaging by smashing method

Take a snapshot

Nuclei collisions

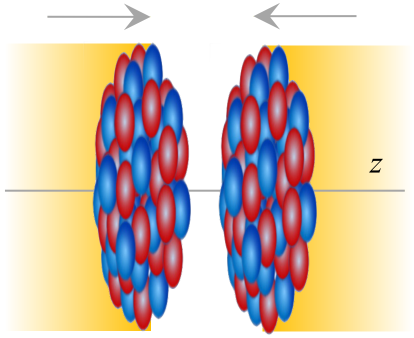

$T_{\mu\nu}(\tau = 0)$

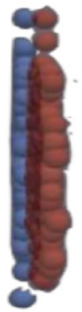

$\tau \sim 2R_0/\Gamma \sim 0.1\text{fm}/c$
exposure

Evolution

$\partial_\mu T^{\mu\nu} = 0$, EOS, viscosity…

Pressure-driven expansion of

Quark-gluon plasma (QGP)

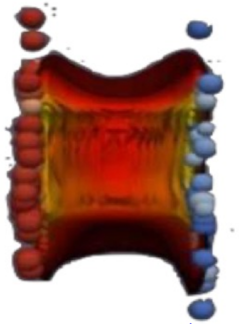

$\tau \sim 10\text{fm}/c$
expansion

free-streaming

Measurement

$T_{\mu\nu}(\tau = \infty)$

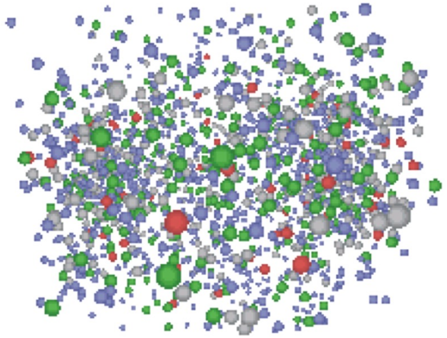

$\tau \sim 10^{15}\text{fm}/c$
detection

$$\rho(r,\theta,\phi) = \frac{\rho_0}{1 + e^{(r-R(\theta,\phi))/a_0}}$$

- $\beta_2 \longrightarrow$ quadrupole deformation
- $\beta_3 \longrightarrow$ octupole deformation
- $\gamma \longrightarrow$ triaxiality
- $a_0 \longrightarrow$ surface diffuseness
- $R_0 \longrightarrow$ nuclear size

ab initio theory/shell model/DFT

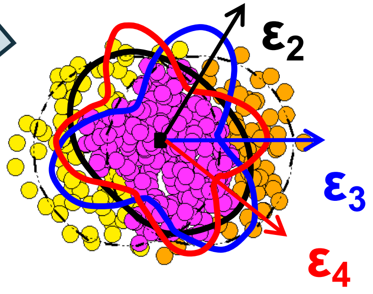

size & shape

$R_\perp^2 \propto \langle r_\perp^2 \rangle$ $\quad$ $\mathcal{E}_n \propto \langle r_\perp^n e^{in\phi} \rangle$

R_0 $\quad$ a_0 $\quad$ β_n

observables

$$\frac{d^2N}{d\phi dp_T} = N(p_T)\left(\sum_n V_n e^{-in\phi}\right)$$

Event-by-event linear responses:

$$\frac{\delta[p_T]}{[p_T]} \propto -\frac{\delta R_\perp}{R_\perp} \qquad V_n \propto \mathcal{E}_n$$

Key: 1) fast snapshot, 2) linear response, 3) large multiplicity for many-body correlation

Linear response in ultra-central collisions

$$\frac{\delta[p_T]}{[p_T]} \propto -\frac{\delta R_\perp}{R_\perp}$$

$$V_n \propto \mathcal{E}_n$$

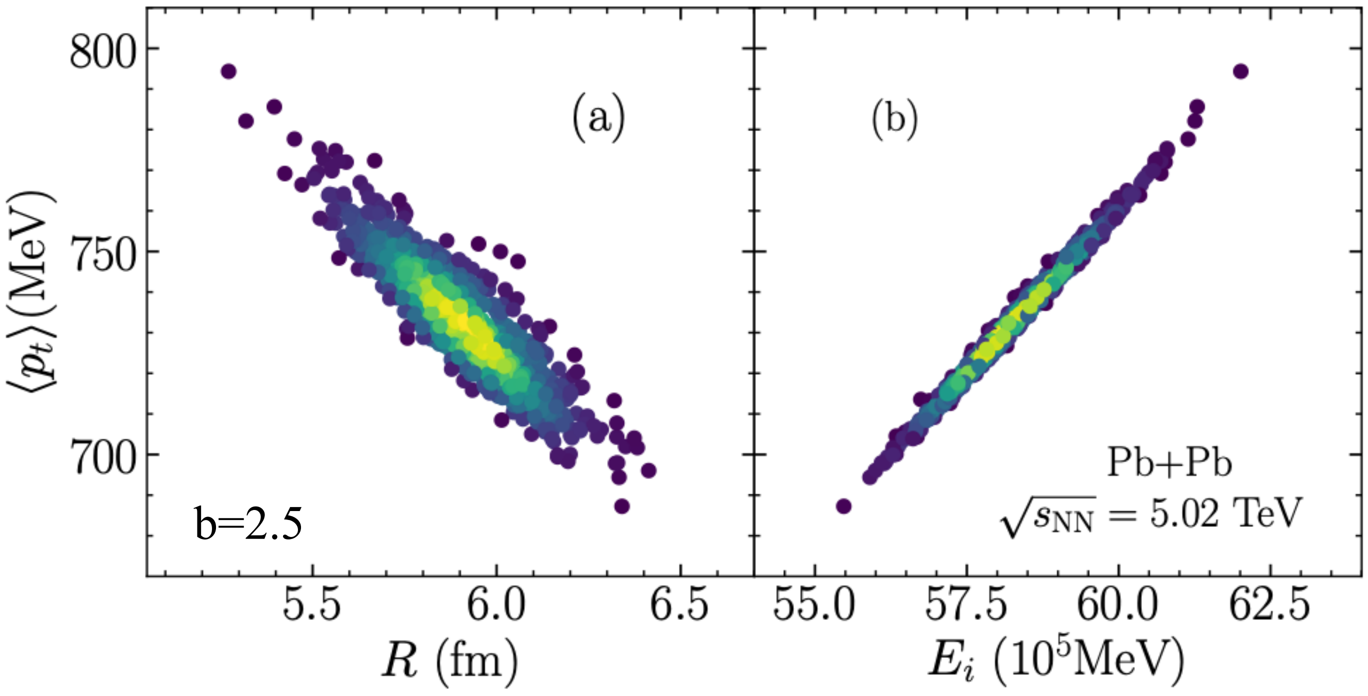

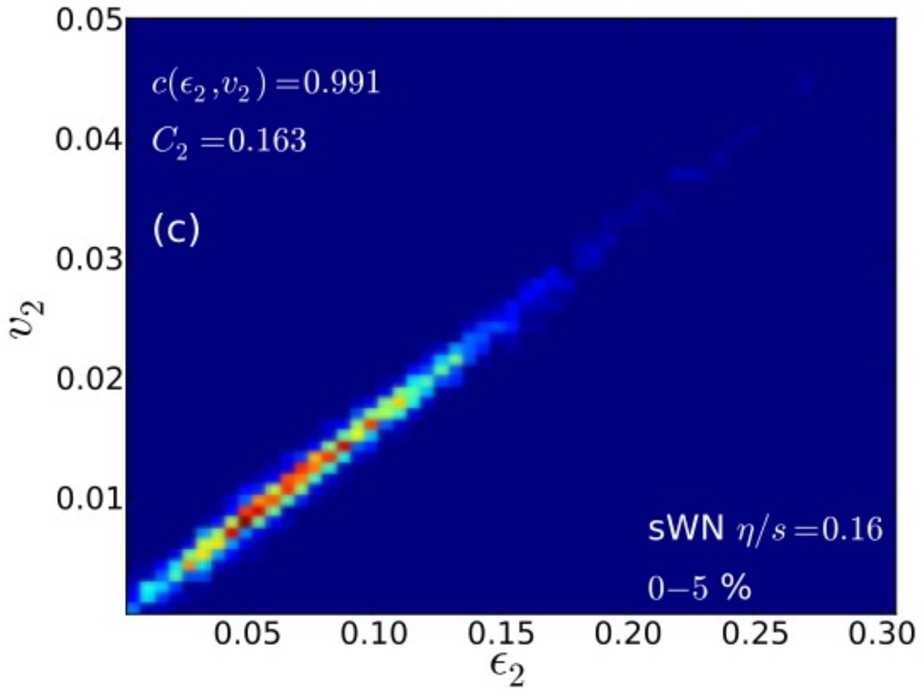

G. Giacalone, F. Gardim, J. Hostler, J. Ollitrault, et al, PRC 103, 024909 (2021)

H. Niemi, G. Denicol, H. Holopainen, P. Huovinen, PRC 87, 054901 (2013)

II. Nuclear deformation in ^{238}U and ^{129}Xe nuclei

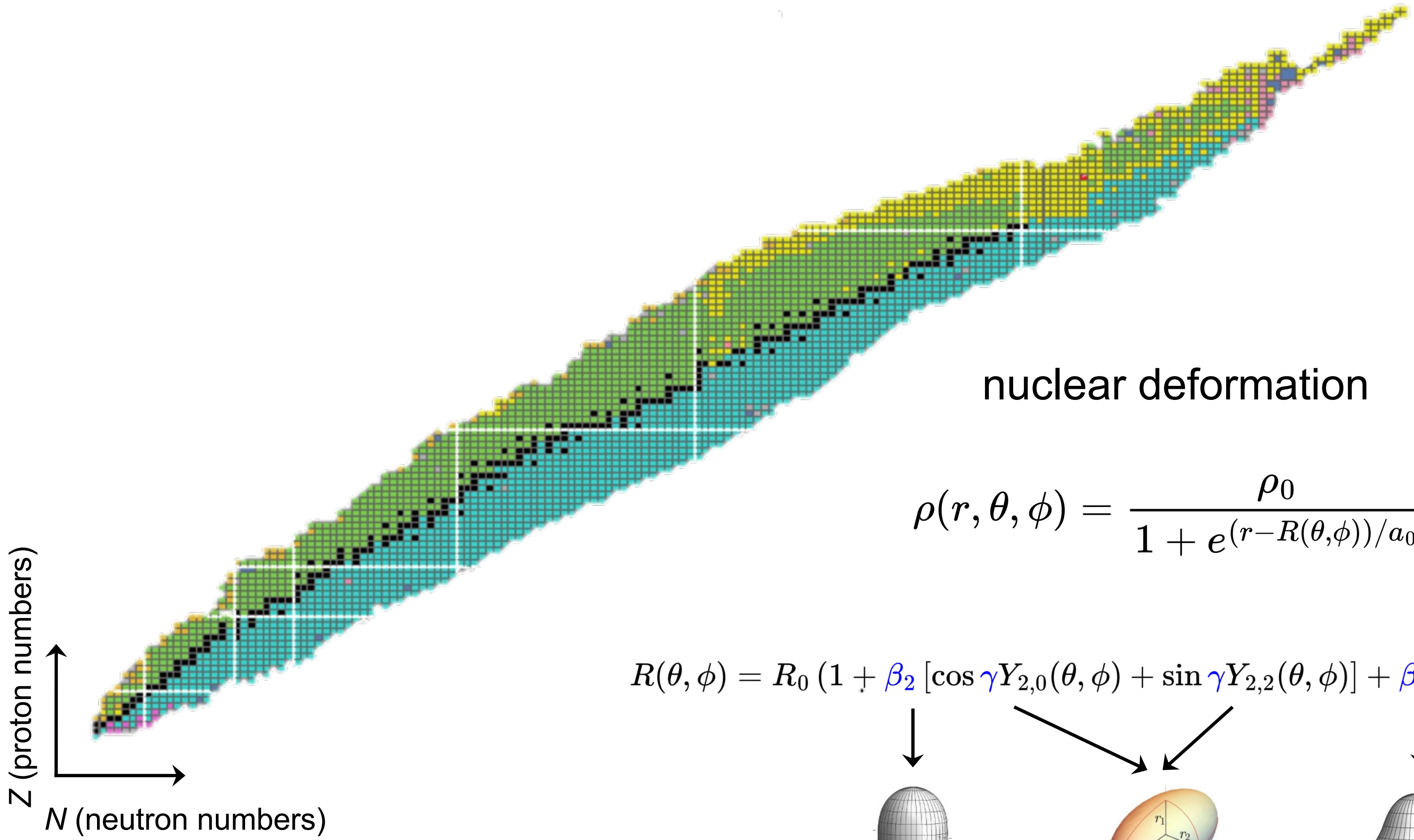

nuclear deformation

$$\rho(r,\theta,\phi) = \frac{\rho_0}{1 + e^{(r-R(\theta,\phi))/a_0}}$$

$$R(\theta,\phi) = R_0\left(1 + \beta_2\left[\cos\gamma Y_{2,0}(\theta,\phi) + \sin\gamma Y_{2,2}(\theta,\phi)\right] + \beta_3 Y_{3,0}(\theta,\phi) + \beta_4 Y_{4,0}(\theta,\phi)\right)$$

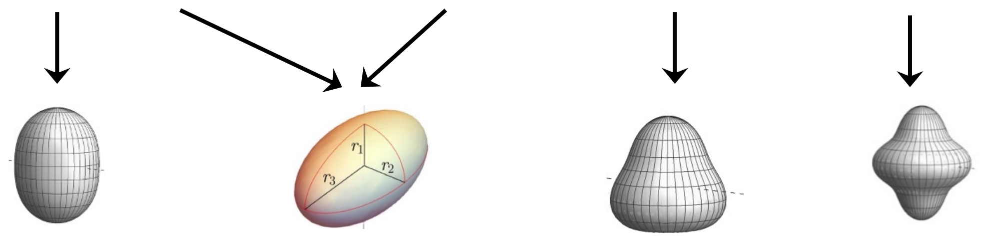

Imaging nuclear shape in high-energy snapshot as a novel way

- Nuclear shape in intrinsic (body-fixed) frame not directly visible in the lab frame

  --Mainly inferred from non-invasive spectroscopy methods.

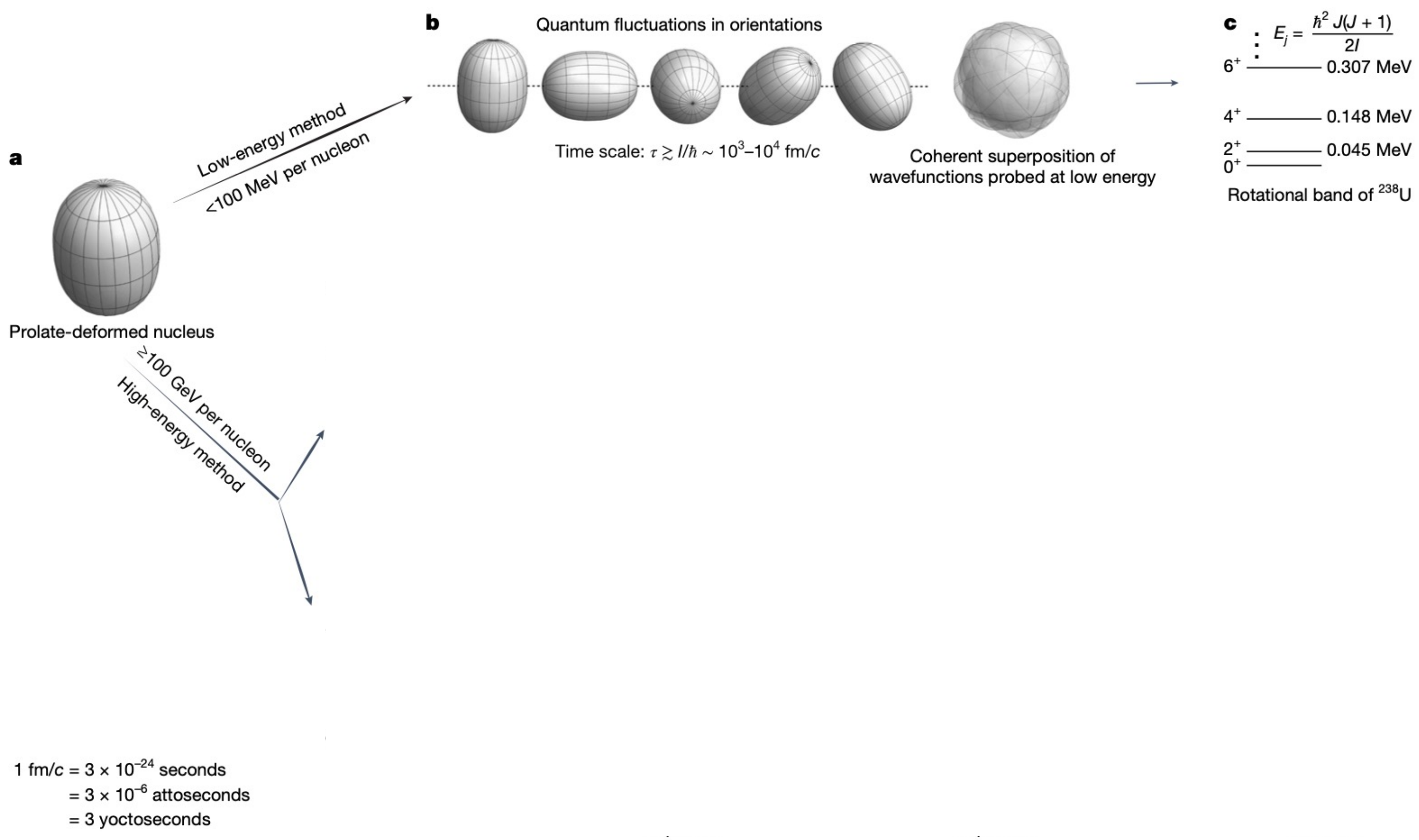

Imaging nuclear shape in high-energy snapshot as a novel way

- Nuclear shape in intrinsic (body-fixed) frame not directly visible in the lab frame

  --Mainly inferred from non-invasive spectroscopy methods.

STAR, Nature 635, 67-72 (2024)

https://www.nature.com/articles/s41586-024-08097-2

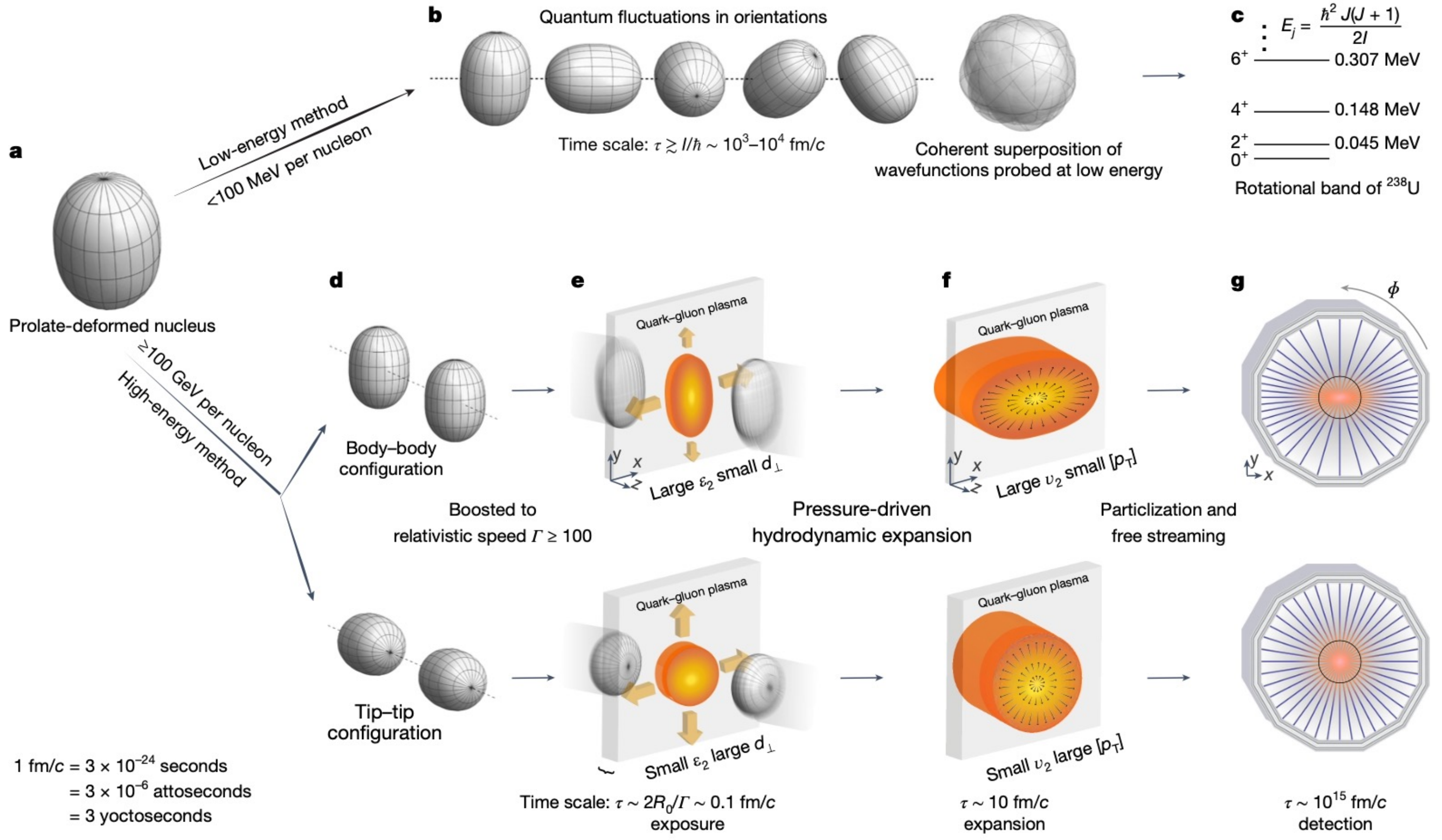

Body-body: large-eccentricity large-size

$v_2 \nearrow \quad p_T \searrow$

Tip-tip : small-eccentricity small-size

$v_2 \searrow \quad p_T \nearrow$

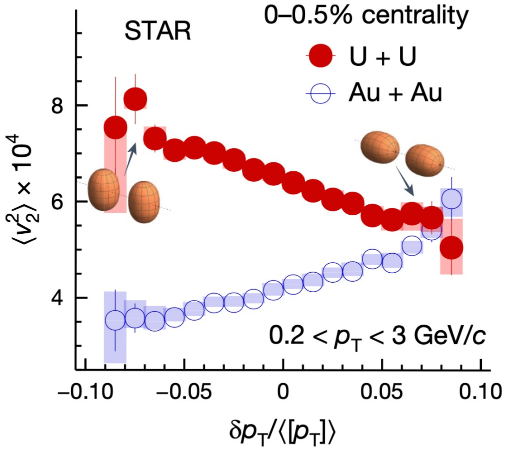

Imaging nuclear shape in high-energy snapshot as a novel way

- Nuclear shape in intrinsic (body-fixed) frame not directly visible in the lab frame
  --Mainly inferred from non-invasive spectroscopy methods.

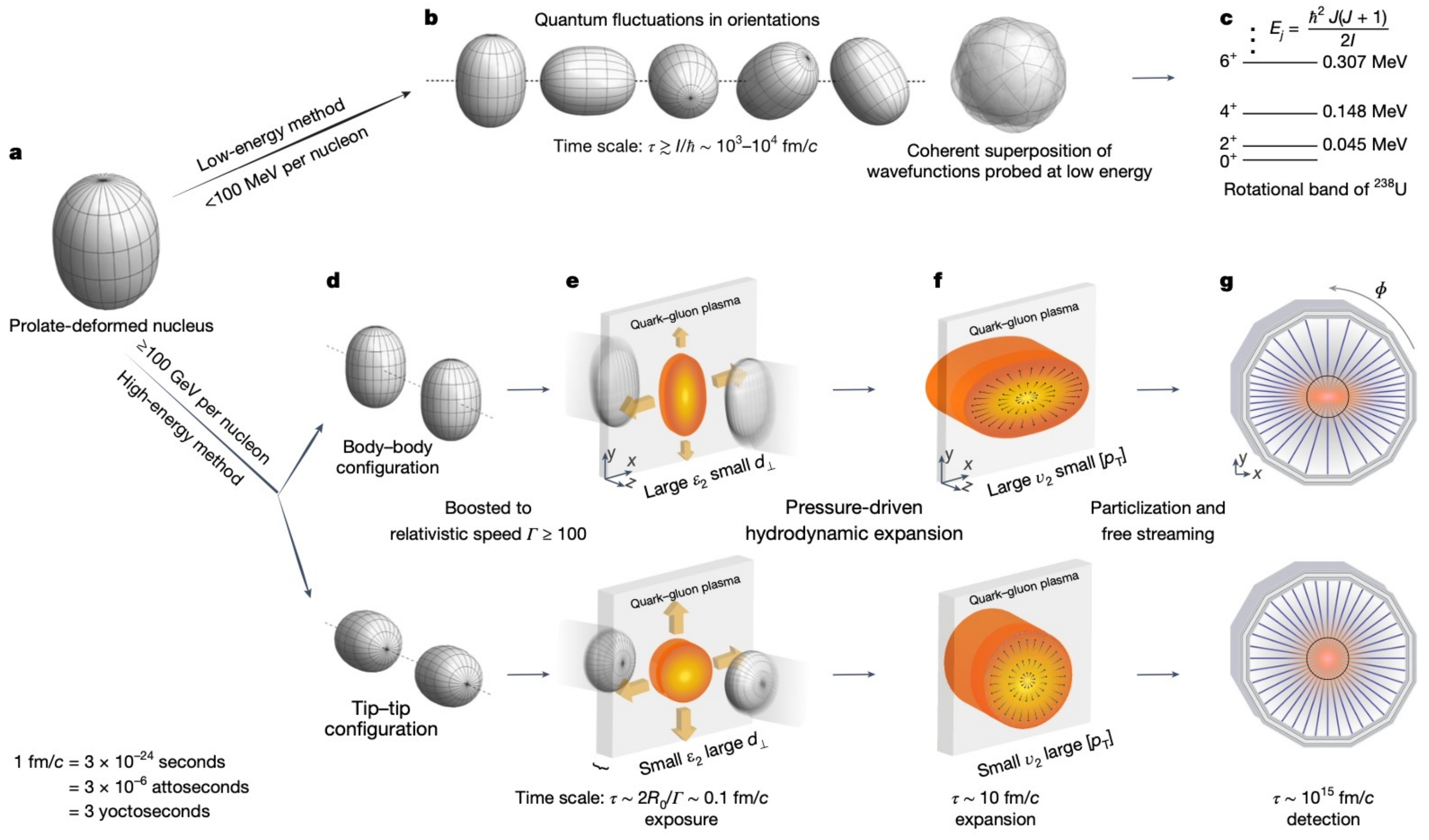

STAR, Nature 635, 67-72 (2024)
https://www.nature.com/articles/s41586-024-08097-2

across energy scales

Body-body: large-eccentricity large-size

$v_2 \nearrow \quad p_T \searrow$

Tip-tip : small-eccentricity small-size

$v_2 \searrow \quad p_T \nearrow$

$$\langle v_2^2 \rangle = a_1 + b_1 \beta_2^2,$$
$$\langle (\delta p_T)^2 \rangle = a_2 + b_2 \beta_2^2,$$
$$\langle v_2^2 \delta p_T \rangle = a_3 - b_3 \beta_2^3 \cos(3\gamma).$$

G. Giacalone, J. Jia, C. Zhang, PRL 127, 242301(2021)

Shape-frozen like a snapshot during nuclear crossing (10^{-25}s << rotational time scale 10^{-21}s)

probe entire mass distribution in the intrinsic frame via multi-point correlations

Ratio of observables

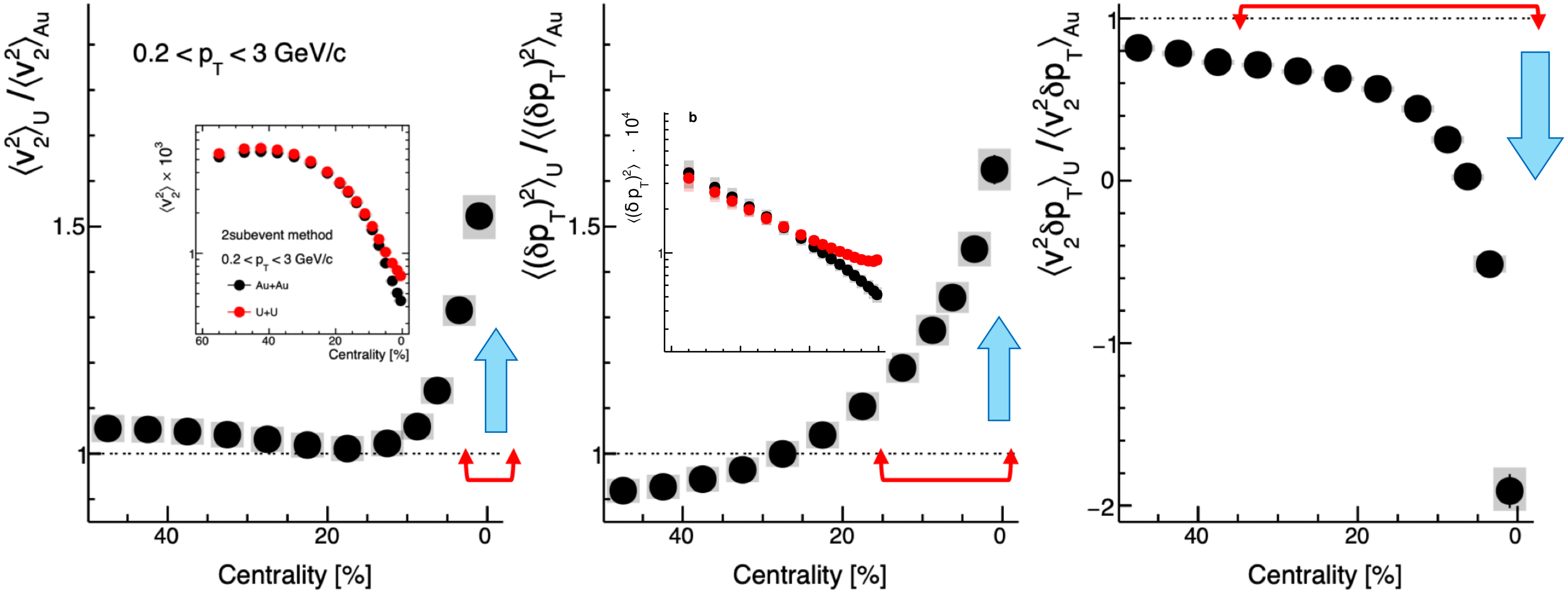

$$R_{\langle v_2^2\rangle} \approx 1 + \frac{b_1}{a_1}\beta_2^2,$$
$$R_{\langle(\delta p_{\mathrm{T}})^2\rangle} \approx 1 + \frac{b_2}{a_2}\beta_2^2,$$
$$R_{\langle v_2^2\delta p_{\mathrm{T}}\rangle} \approx 1 - \frac{b_3}{a_3}\beta_2^3\cos(3\gamma)$$

- Elliptic flow and size fluctuation are enhanced by the nuclear deformation effect.
- Ratios cancel final state effects and isolate the effects of initial state/nuclear structures.

→ U deformation dominates the ultra-central collisions (UCC)

Constraining the ground-state ^{238}U: β_2 and γ

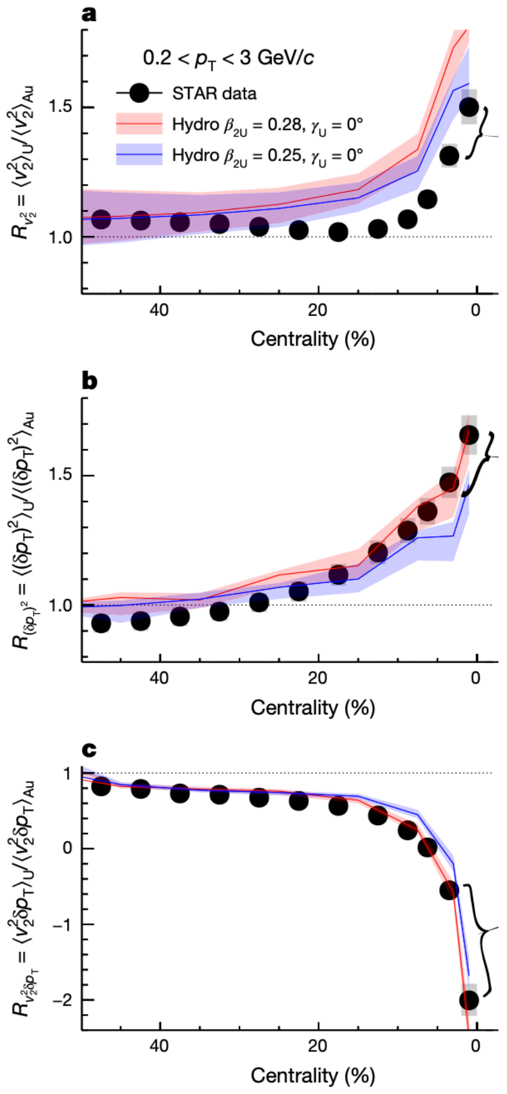

Constraining the ground-state ^{238}U: β_2 and γ

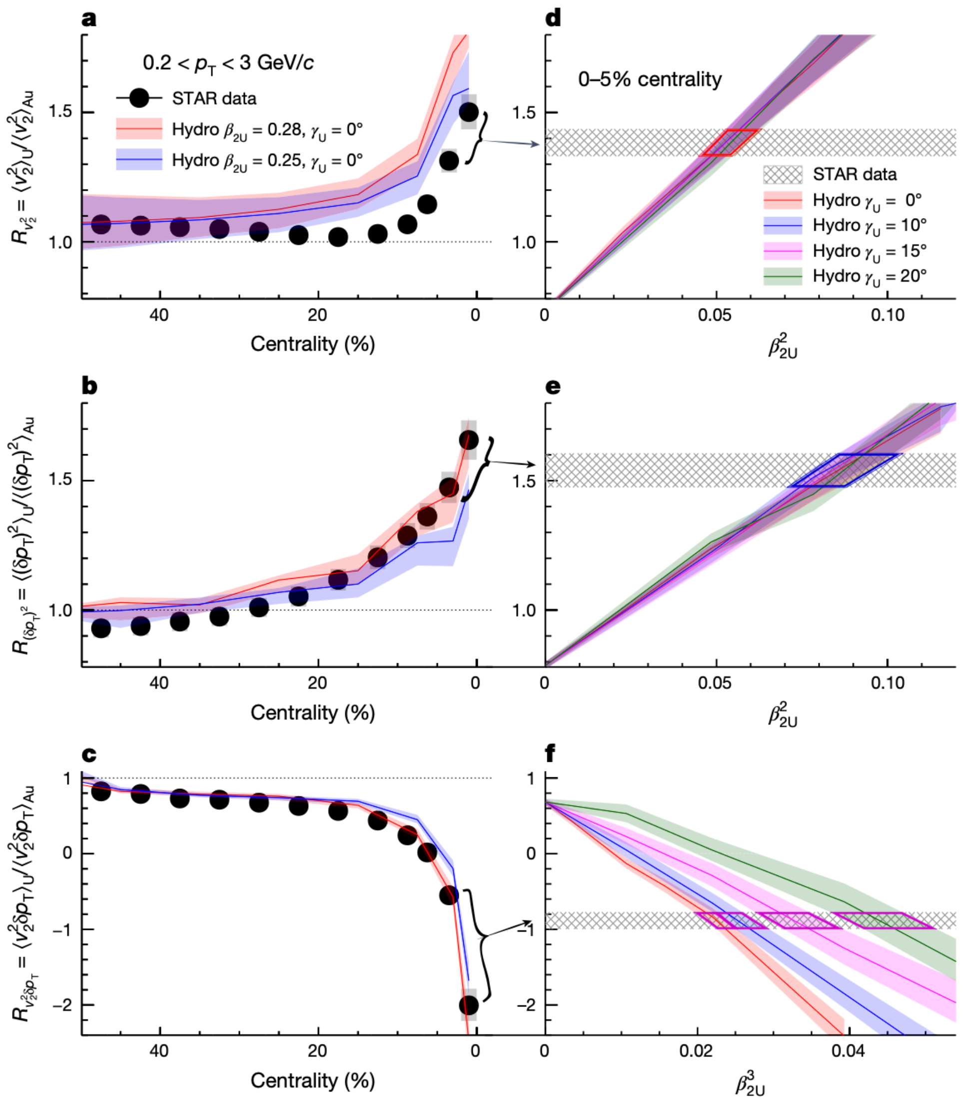

Sufficient precision is achieved from ratios in ultra-central collisions

Relation confirmed from hydro

$$R_{\langle v_2^2 \rangle} \approx 1 + \frac{b_1}{a_1}\beta_2^2,$$
$$R_{\langle (\delta p_T)^2 \rangle} \approx 1 + \frac{b_2}{a_2}\beta_2^2,$$
$$R_{\langle v_2^2 \delta p_T \rangle} \approx 1 - \frac{b_3}{a_3}\beta_2^3 \cos(3\gamma)$$

Constraining the ground-state ^{238}U: β_2 and γ

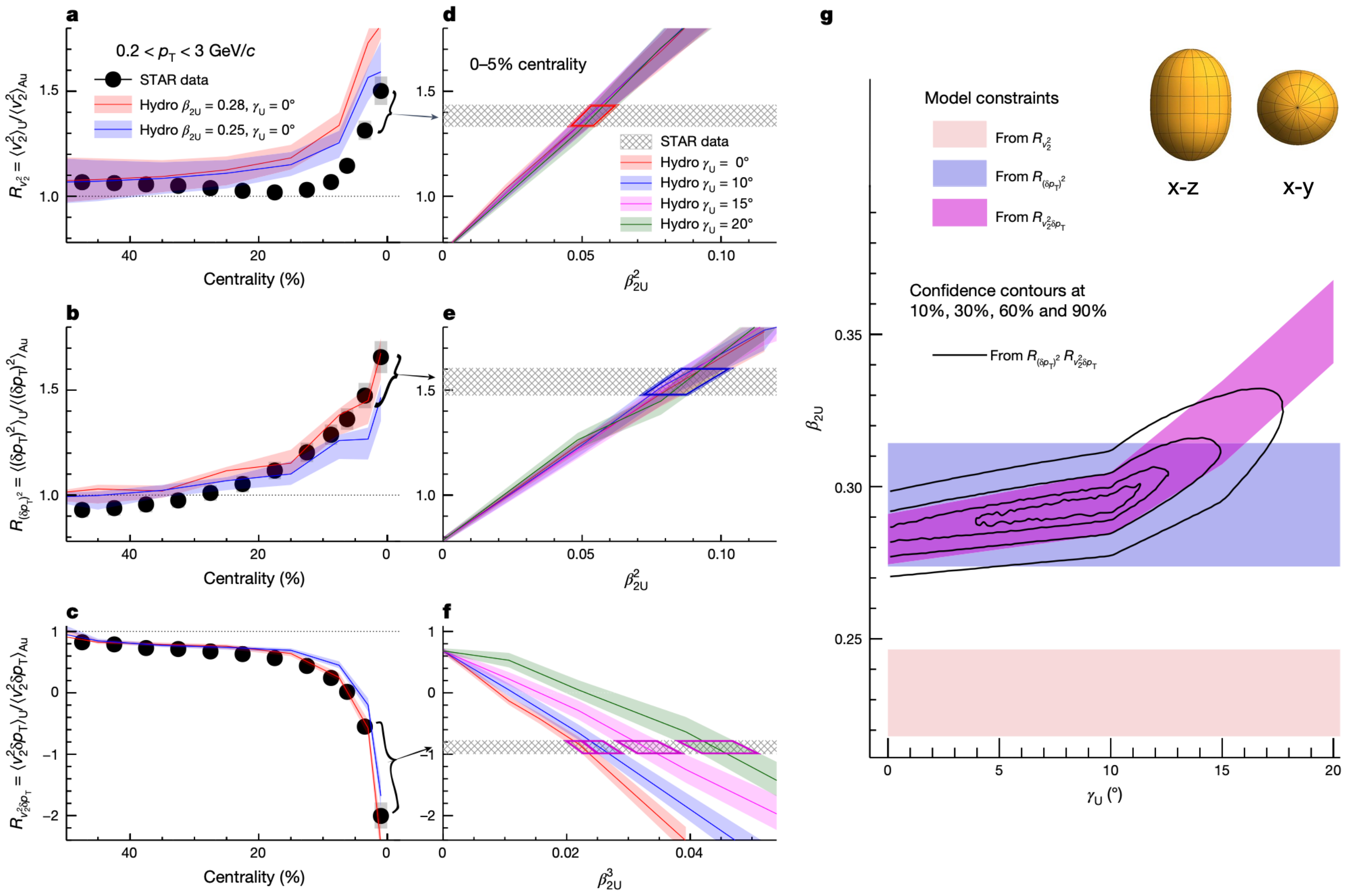

Sufficient precision is achieved from ratios in ultra-central collisions

Relation confirmed from hydro

$$R_{\langle v_2^2\rangle} \approx 1 + \frac{b_1}{a_1}\beta_2^2,$$
$$R_{\langle(\delta p_T)^2\rangle} \approx 1 + \frac{b_2}{a_2}\beta_2^2,$$
$$R_{\langle v_2^2 \delta p_T\rangle} \approx 1 - \frac{b_3}{a_3}\beta_2^3\cos(3\gamma)$$

High-energy estimate:

$$\beta_{2\mathrm{U}} = 0.286 \pm 0.025$$
$$\gamma_U = 8.5^\circ \pm 4.8^\circ$$

low-energy estimate:

$$\beta_{2\mathrm{U}} = 0.287 \pm 0.007$$
$$\gamma_U = 6^\circ - 8^\circ$$

A large deformation with a slight deviation from axial symmetry in the nuclear ground-state

Viscosity, nuclear parameters, and model variations

1) Taking the ratios cancels the viscosity effects.

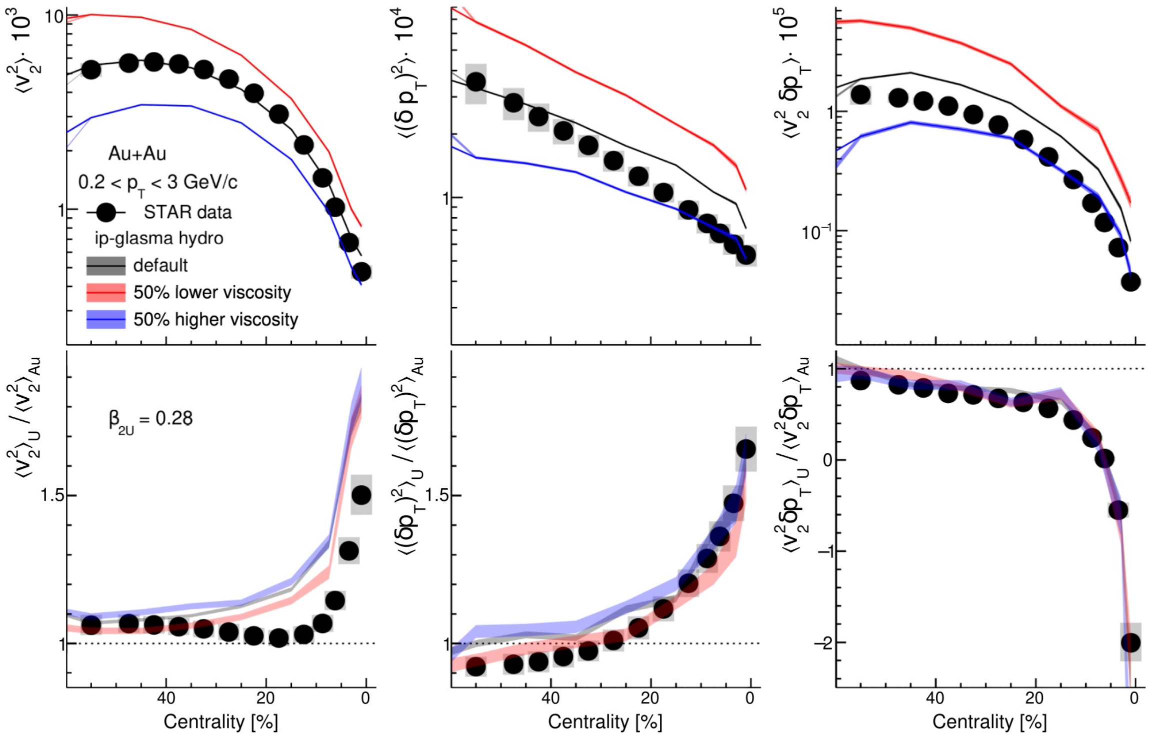

Viscosity, nuclear parameters, and model variations

2) Effect from nuclear parameters are small, included as model systematics.

1) Taking the ratios cancels the viscosity effects.

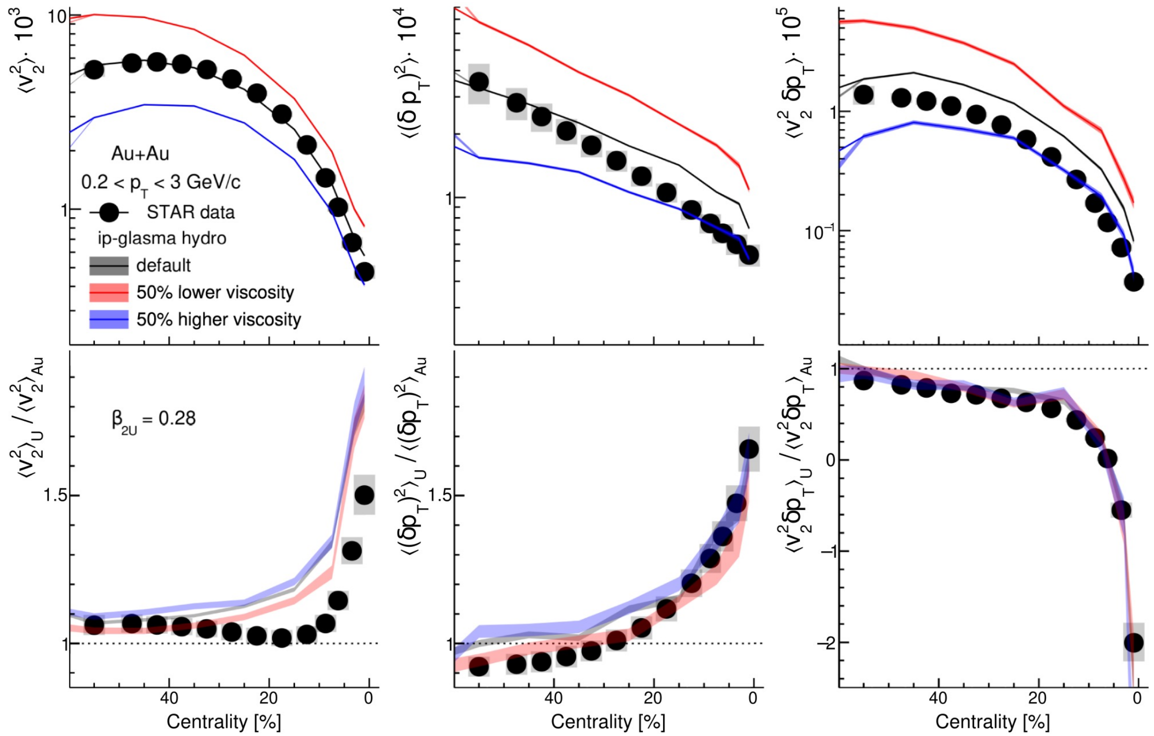

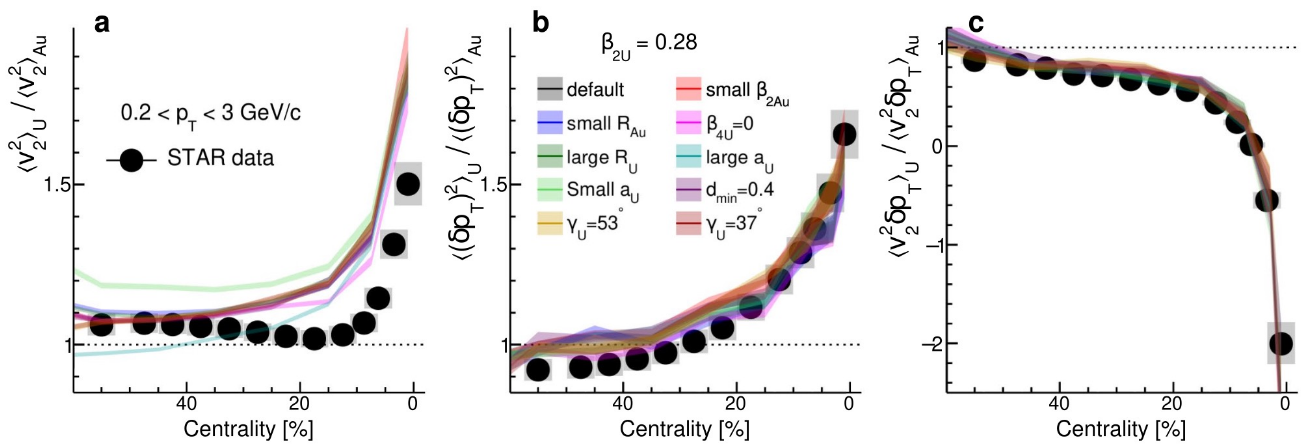

Viscosity, nuclear parameters, and model variations

2) Effect from nuclear parameters are small, included as model systematics.

1) Taking the ratios cancels the viscosity effects.

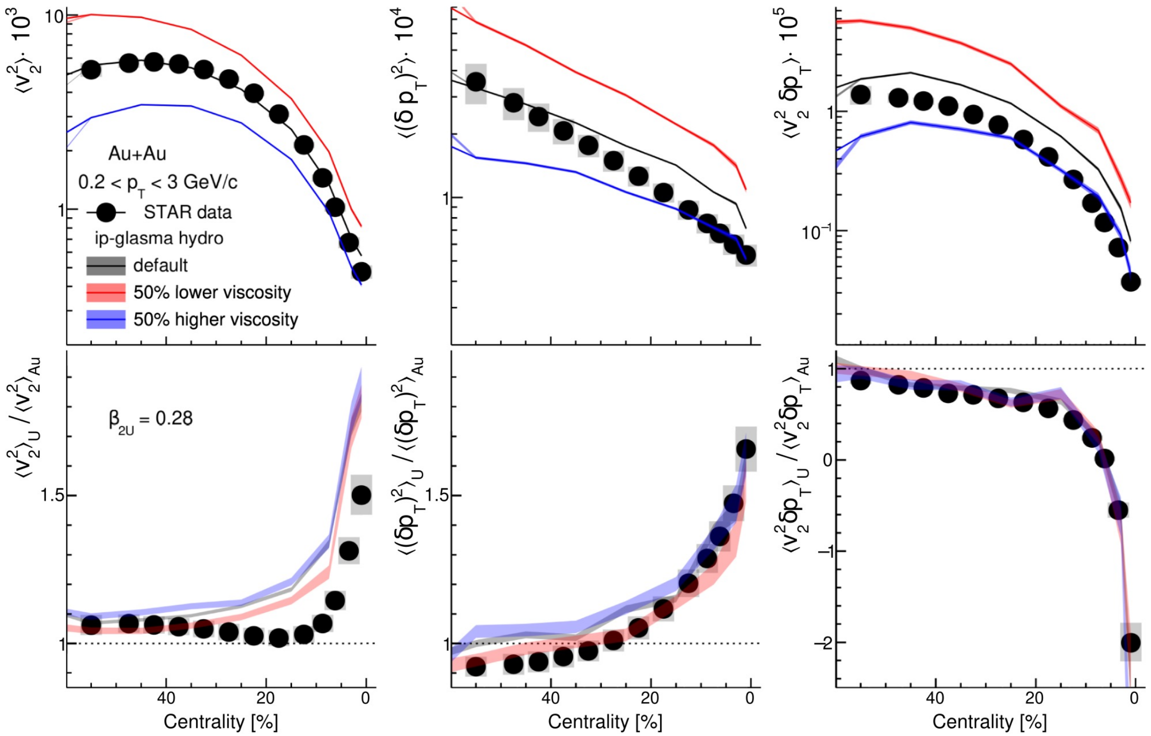

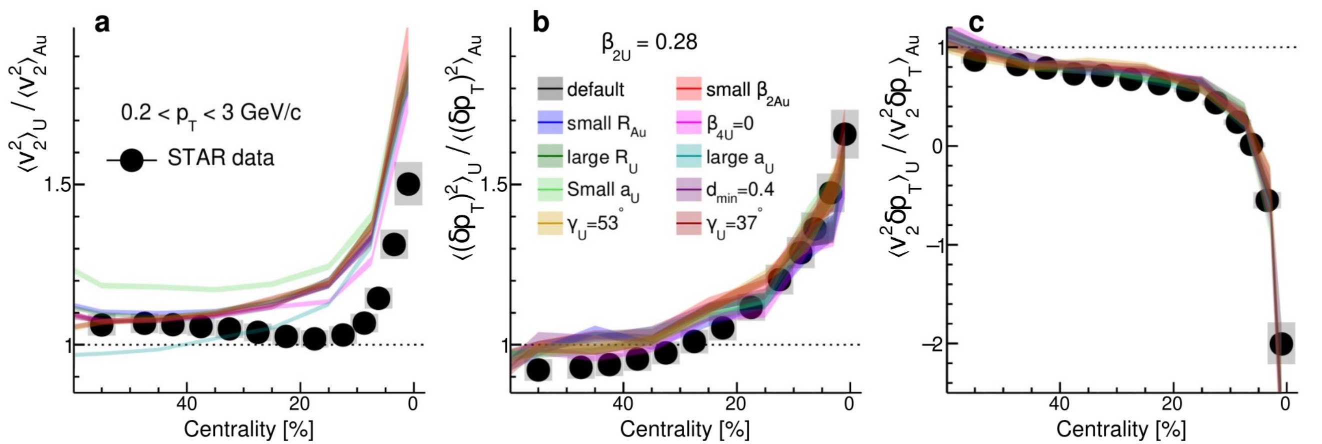

3) Another hydrodynamics model, Trajectum, shows rather consistent extractions even if it was not tuned to RHIC data.

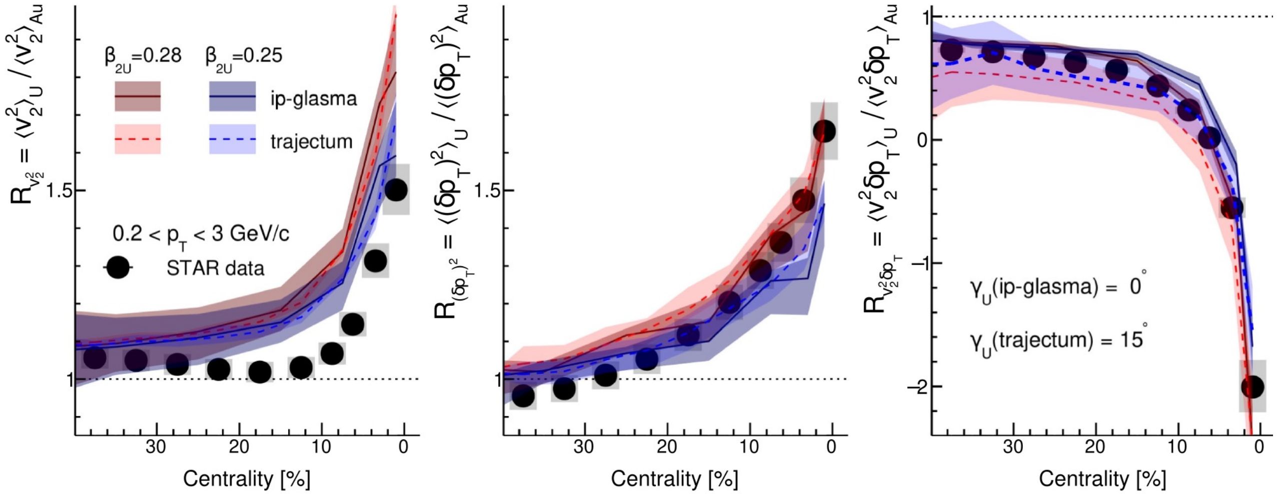

Extracted $\beta_{2,\mathrm{U}}$ and γ_{U} values are robust.

[p_T] fluctuations as other novel tool

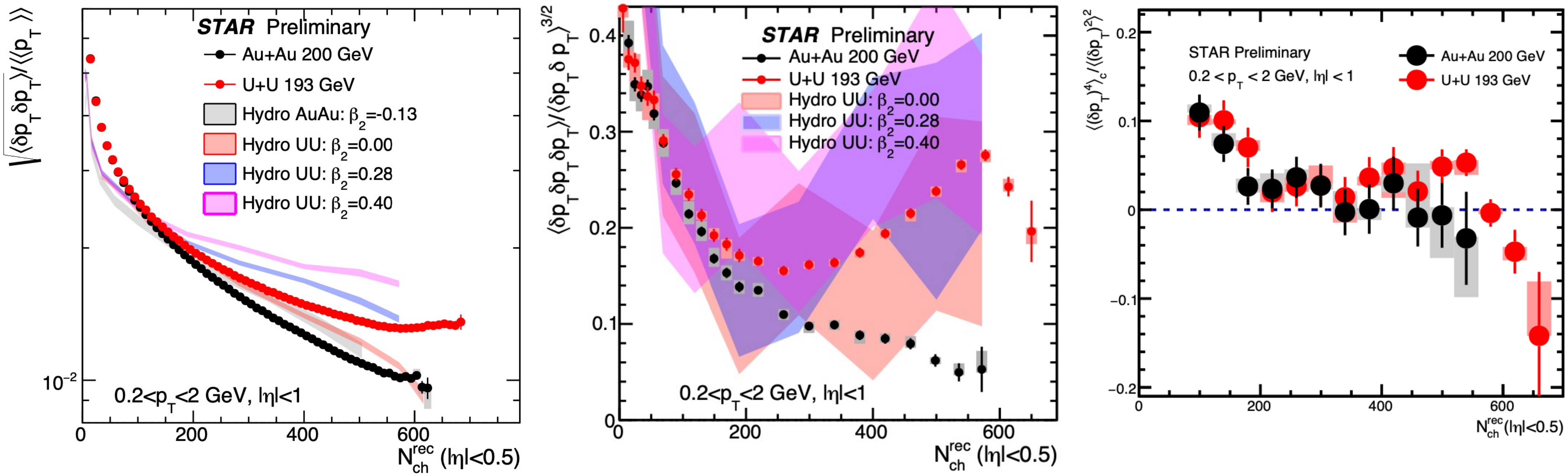

Au+Au: variance and skewness follow independent source scaling $1/N_s^{n-1}$ within power-law decrease

U+U: large enhancement in normalized variance and skewness and sign-change in normalized kurtosis
⟶ size fluctuations enhanced

The nuclear deformation role is further confirmed by hydro calculations. But we need more statistics.

[p_T] fluctuations also serve as a good observable to explore the role of nuclear deformation.

ALICE, PLB 850, 138541 (2024); ATLAS, PRL 133, 252301 (2024)

Evidence of octupole deformation $\beta_{3,\mathrm{U}}$

EDMs search

Octupole deformation enhanced atomic EDM moment

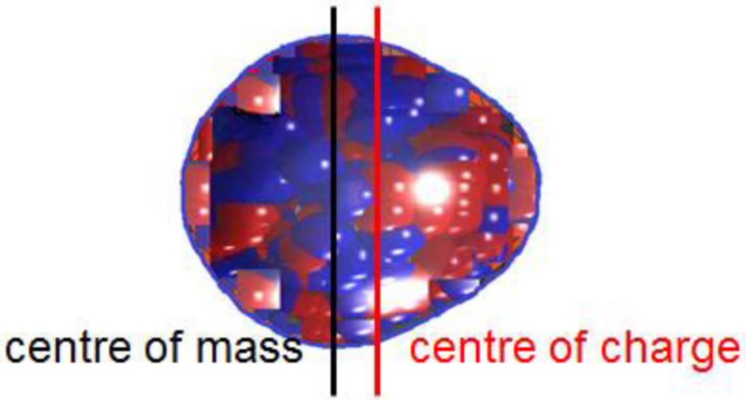

finite size and shape of nucleus breaks the symmetry

Higher sensitivity via Schiff nuclear moments in heavy nuclei

Octupole collectivity

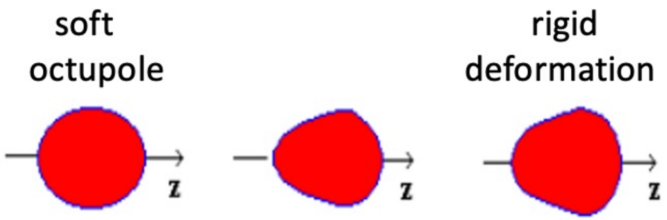

Nature 497, 199 (2013); Rev. Mod. Phys. 91, 015001 (2019);
Rep. Prog. Phys. 80, 046301 (2017); Ann. Rev. Nucl. Part. Sci. 69, 219 (2019);

Evidence of octupole deformation $\beta_{3,\mathrm{U}}$

EDMs search

Octupole deformation enhanced atomic EDM moment

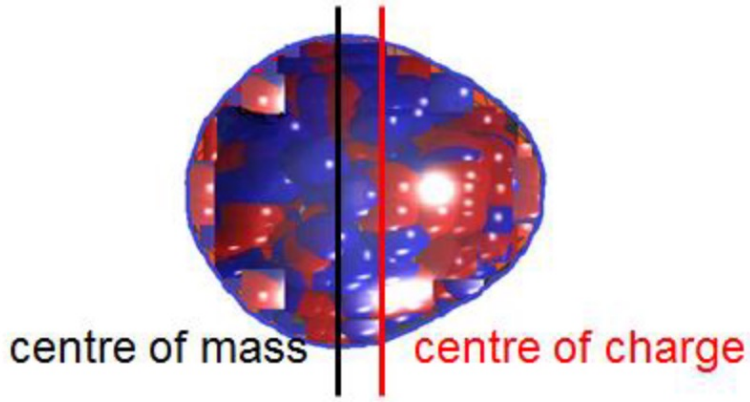

finite size and shape of nucleus breaks the symmetry

Higher sensitivity via Schiff nuclear moments in heavy nuclei

Octupole collectivity

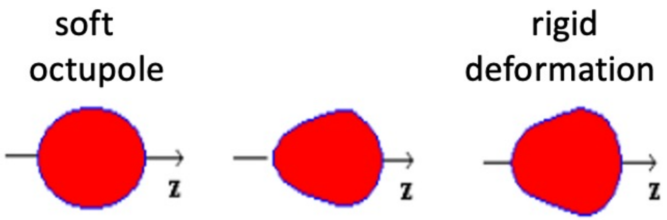

Nature 497, 199 (2013); Rev. Mod. Phys. 91, 015001 (2019);
Rep. Prog. Phys. 80, 046301 (2017); Ann. Rev. Nucl. Part. Sci. 69, 219 (2019);

Neutrinoless double beta decay

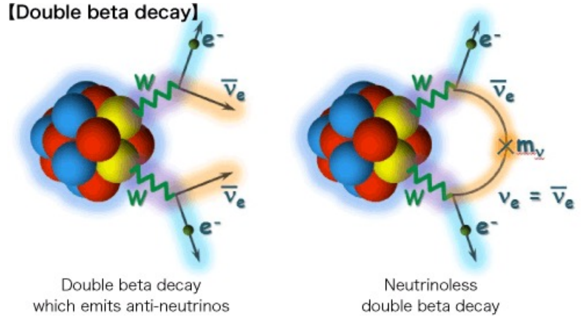

$$T^{0\nu}_{1/2} = \left(G|\mathcal{M}|^2 \langle m_{\beta\beta}\rangle^2\right)^{-1} \simeq 10^{27-28}\left(\frac{0.01\mathrm{eV}}{\langle m_{\beta\beta}\rangle}\right)^2 \mathrm{y}$$

Nuclear Matrix Element

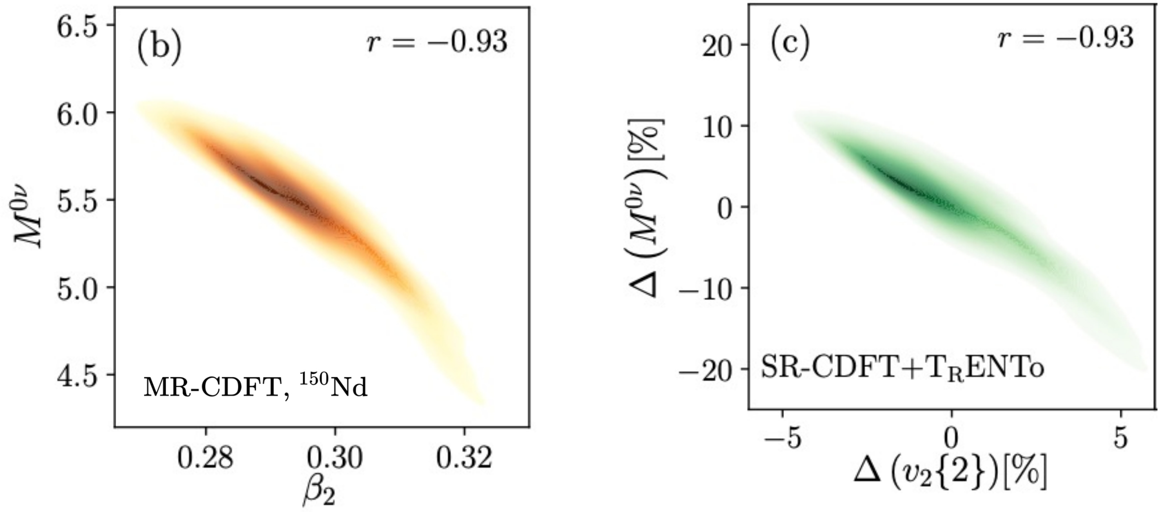

Y. Li, X. Zhang, G. Giacalone, J.M. Yao, PRL 135, 022301 (2025)

Heavy-ion involving 0vββ decay candidates as a platform for benchmarking theoretical predictions of the NME.

Evidence of octupole deformation $\beta_{3,\mathrm{U}}$

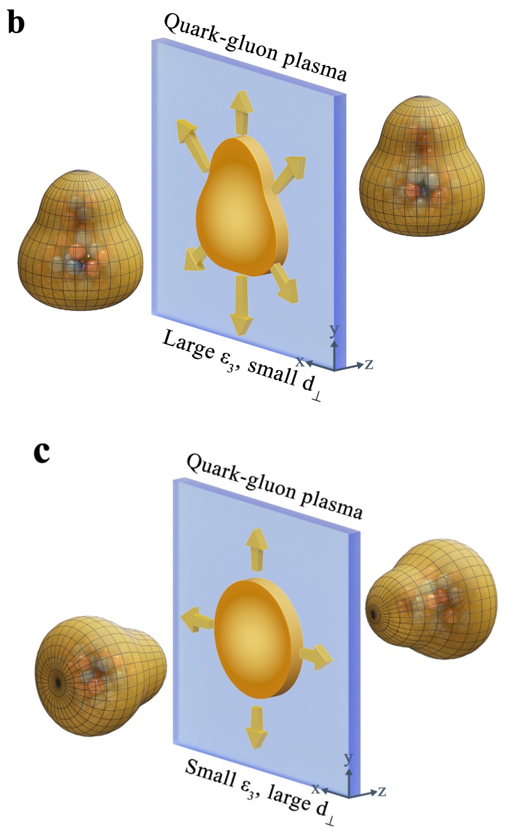

However, v_3 is fluctuation driven, expect in central

$$\langle v_3^2 \rangle \propto \langle \varepsilon_3^2 \rangle \sim 1/A$$

mass number

B. Alver and G. Roland, PRC 81, 054905 (2010)

Evidence of octupole deformation $\beta_{3,\mathrm{U}}$

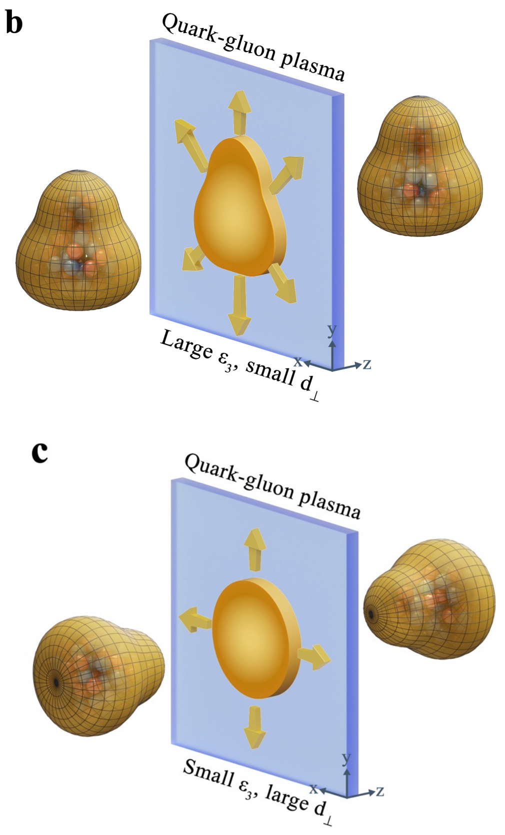

IP-Glasma+MUSIC calculations

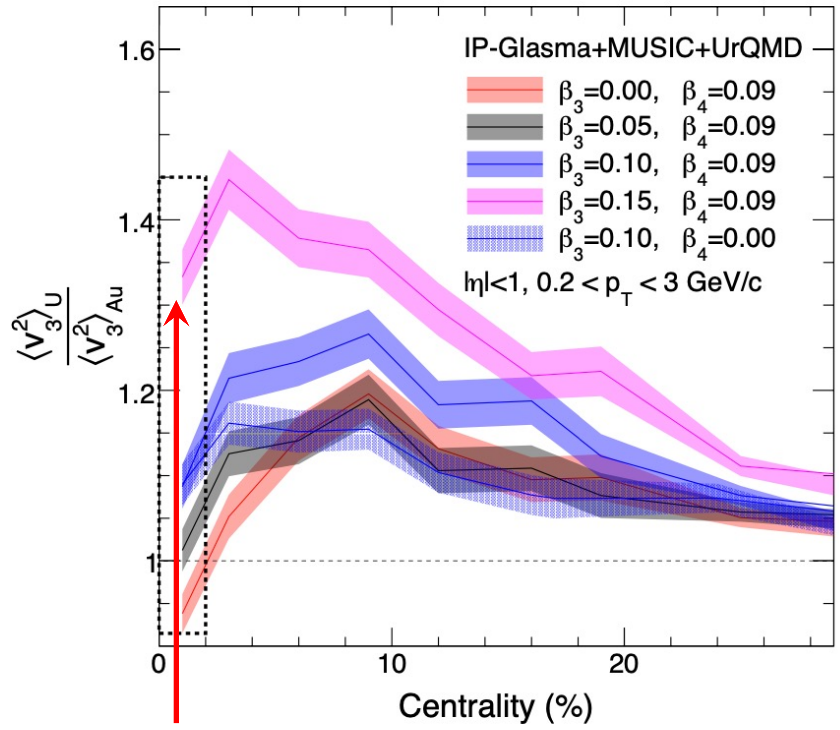

C. Zhang, J. Jia, J. Chen, C. Shen, L. Liu, arXiv: 2504.15245

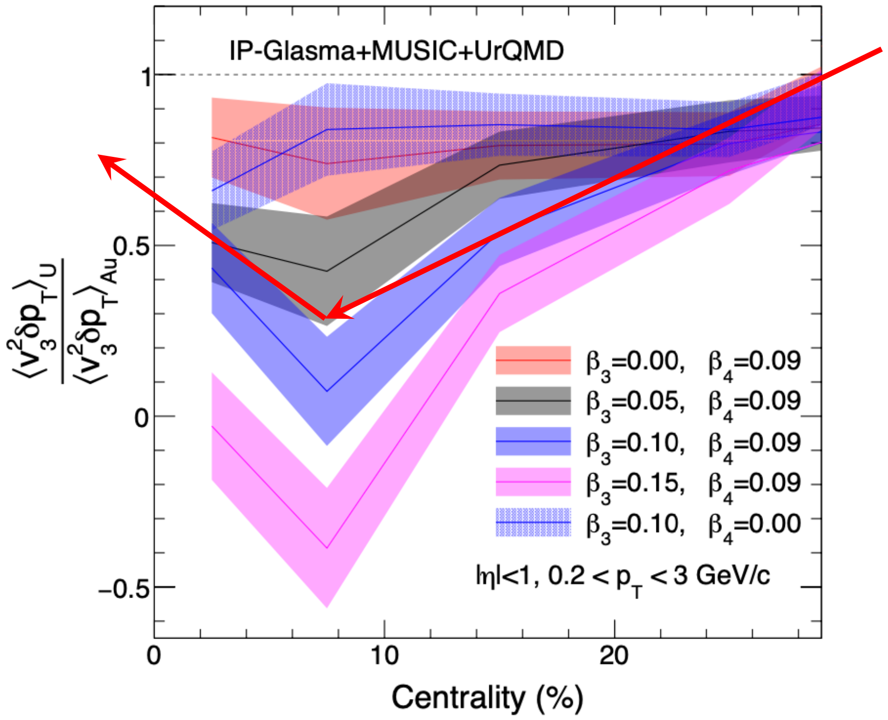

$$R_{v_3^2} = \frac{\langle v_3^2\rangle_{\mathrm{U+U}}}{\langle v_3^2\rangle_{\mathrm{Au+Au}}} \approx \frac{a_{3\mathrm{U}}}{a_{3\mathrm{Au}}} + \frac{b_{3,3}}{a_{3\mathrm{Au}}}\beta_3^2 + \frac{b_{3,4}}{a_{3\mathrm{Au}}}\beta_4^2,$$

$$R_{v_3^2\delta p_T} = \frac{\langle v_3^2\delta p_{\mathrm{T}}\rangle_{\mathrm{U+U}}}{\langle v_3^2\delta p_{\mathrm{T}}\rangle_{\mathrm{Au+Au}}} \approx a - b\beta_2\beta_3^2.$$

However, v_3 is fluctuation driven, expect in central

$$\langle v_3^2\rangle \propto \langle \varepsilon_3^2\rangle \sim 1/A$$

mass number

$\langle v_3^2\rangle$ follows a linear increase with β_3^2,

Characteristic anticorrelation in $\langle v_3^2\delta p_{\mathrm{T}}\rangle$ shows a pronounced β_3-dependent suppression.

B. Alver and G. Roland, PRC 81, 054905 (2010)

Evidence of octupole deformation $\beta_{3,\mathrm{U}}$

STAR, arXiv: 2506.17785, Under Review

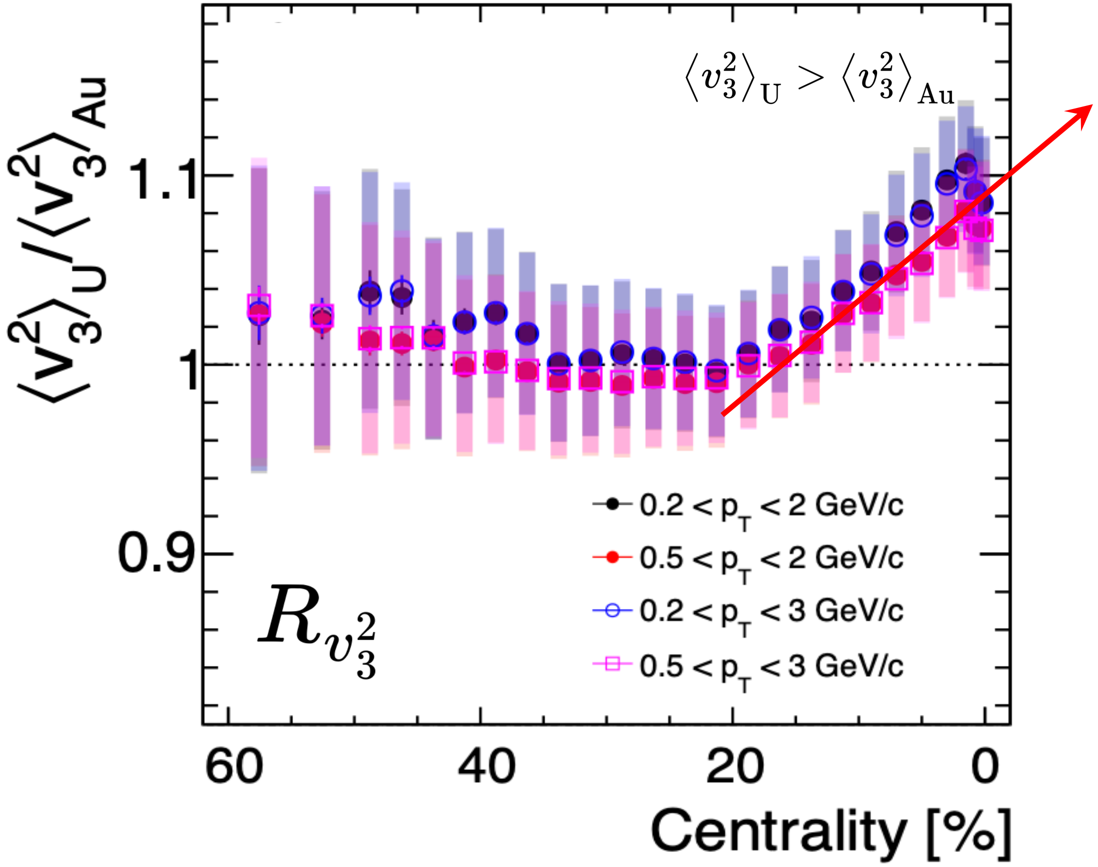

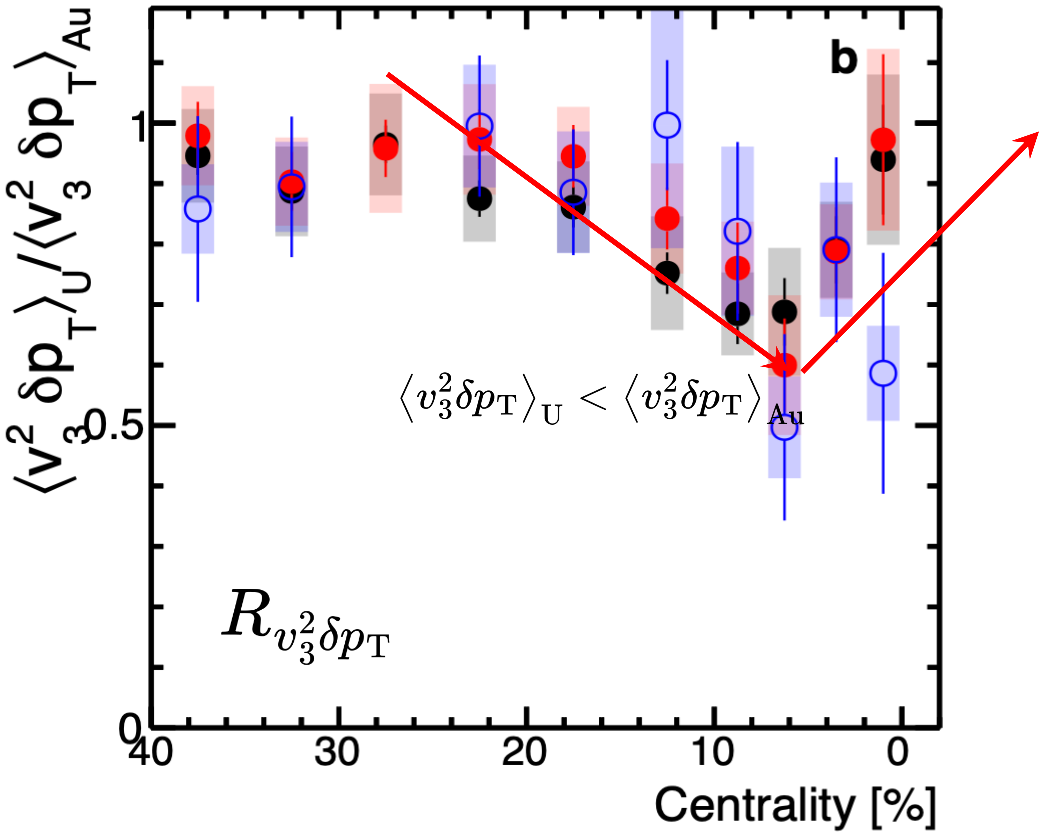

Order of v_3 and v_3-p_T reversed by considering non-zero $\beta_{3,\mathrm{U}}$, $\beta_{4,\mathrm{U}}$.

An evidence and modest $\beta_{3,\mathrm{U}} \sim 0.08$-$0.10$ are confirmed.

Probe $\beta_{3,\mathrm{U}}$ and its fluctuation

Octupole collectivity

L. Liu, C. Zhang, J. Chen, J. Jia, X. Huang, Y. Ma, to appear

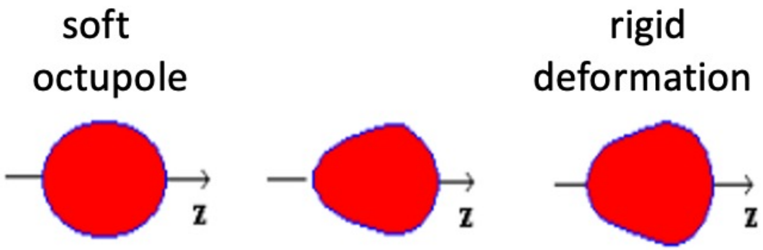

$$\langle \beta_3^2 \rangle = \bar{\beta}_3^2 + \sigma_{\beta_3}^2$$

$$c_{n,\varepsilon}\{2\} = \langle \varepsilon_n^2 \rangle \approx \langle \varepsilon_{n,0}^2 \rangle + \langle p_n p_n^* \rangle \langle \beta_n^2 \rangle$$

$$c_{n,\varepsilon}\{4\} = \langle \varepsilon_n^4 \rangle - 2\langle \varepsilon_n^2 \rangle^2$$
$$\approx \langle \varepsilon_{n,0}^4 \rangle - 2\langle \varepsilon_{n,0}^2 \rangle^2 + \langle p_n^2 p_n^{2*} \rangle \langle \beta_n^4 \rangle - 2\langle p_n p_n^* \rangle^2 \langle \beta_n^2 \rangle^2$$

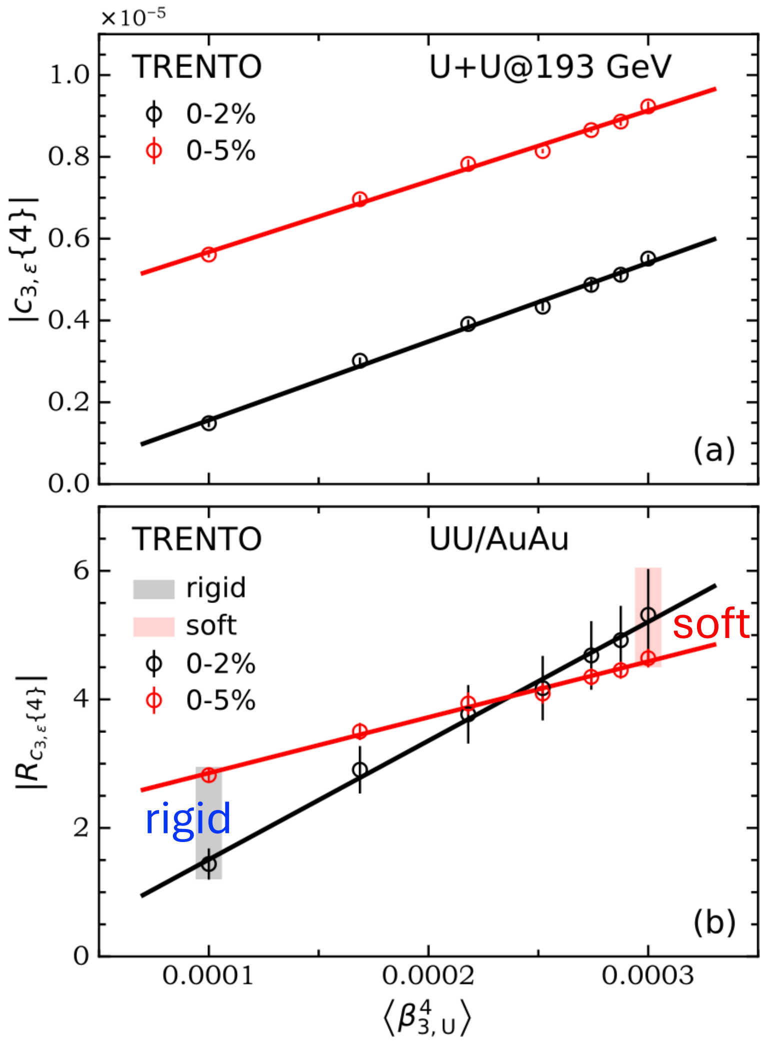

Four-particle correlation is linearly scaled to $\langle \beta_{3,\mathrm{U}}^4 \rangle$.

A way to discriminate between static and dynamic collective modes in high-energy nuclear collisions

Constraint on hexadecapole deformation $\beta_{4,U}$

H. Xu, J. Zhao, F. Wang, PRL132, 262301 (2024)
Z. Wang. J. Chen, H. Xu, J. Zhao, PRC 110, 034907 (2024)

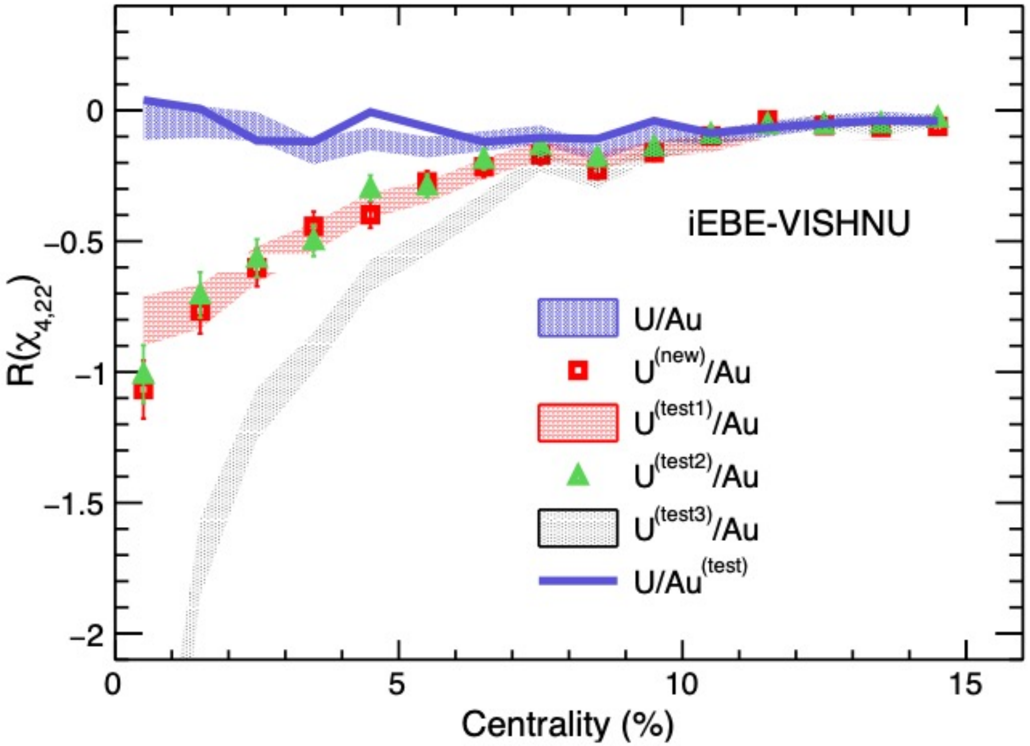

Non-linear response coefficient is sensitive to the $\beta_{4,\mathrm{U}}$

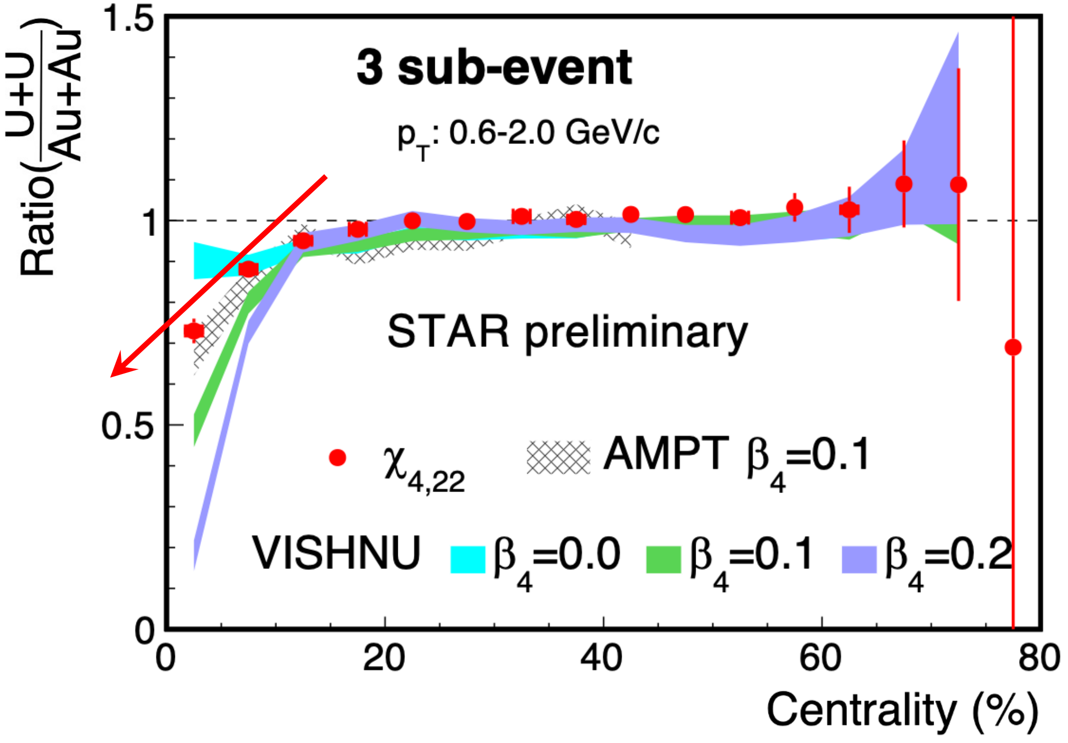

$\beta_{4,\mathrm{U}}$ constrained using $\chi_{4,22}$ ratio in the central region

VISHNU overpredicts the data but AMPT prediction is well

W. Ryssens, G. Giacalone, B. Schenke, C. Shen, PRL 130, 212302 (2023)

Triaxial structure of ^{129}Xe at LHC

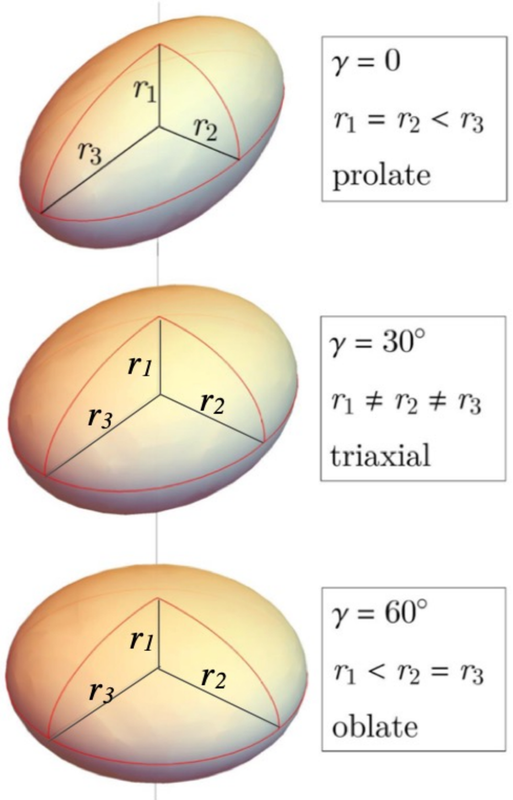

ALICE, PLB 834, 137393 (2022)

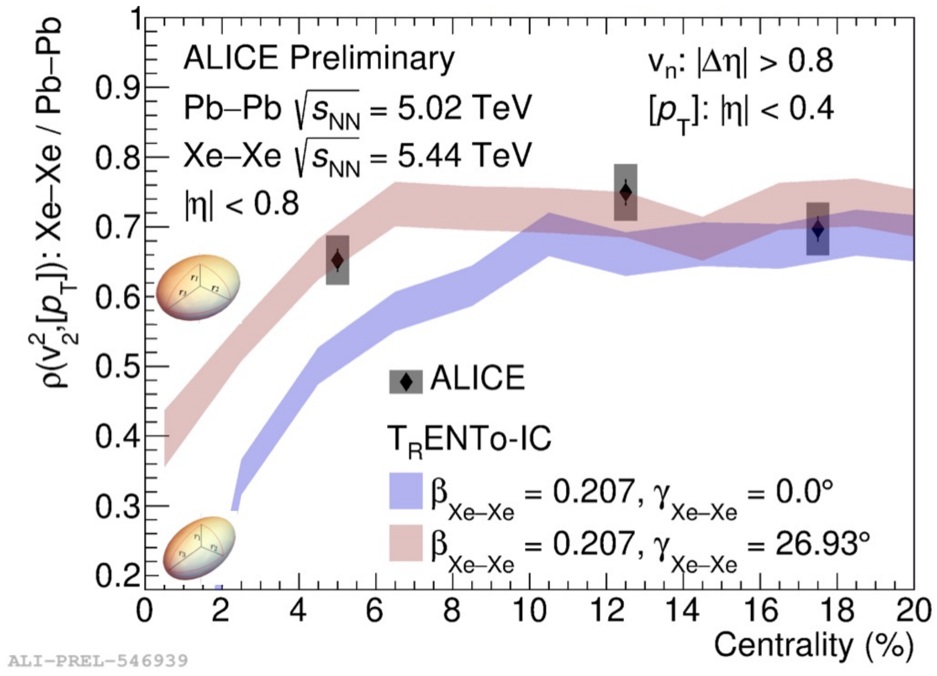

ATLAS, PRC 107, 054910 (2023)

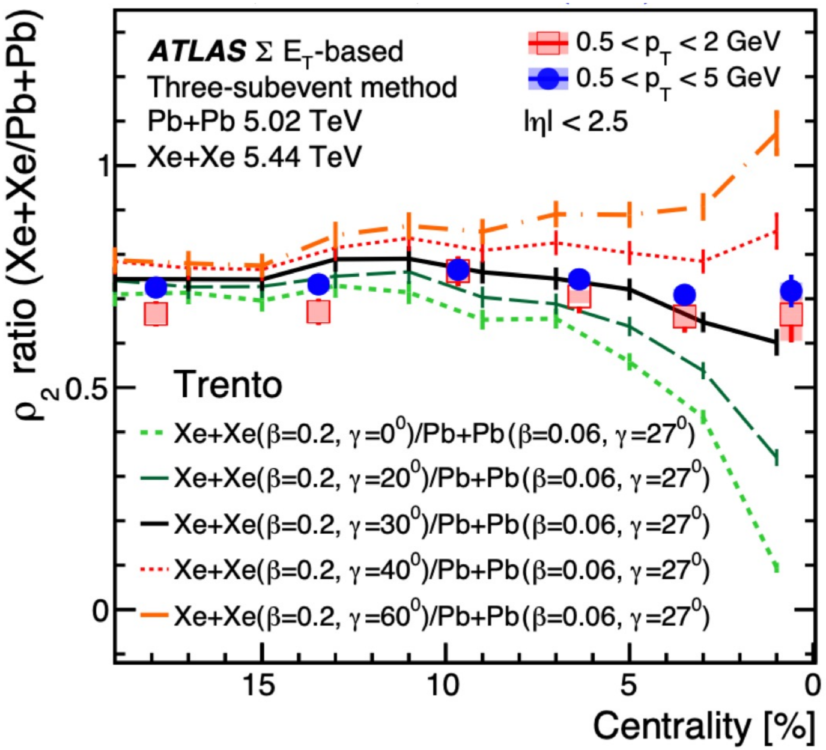

Better agreement between LHC data and calculations with γ = 27°-30° (triaxial)
→ First study of triaxial structure of ^{129}Xe at high-energy collisions at the LHC
→ Evidence of triaxial structure of ^{129}Xe? γ fluctuation?

B. Bally etc, PRL128, 082301 (2022); S. Zhao, H. Xu, Y. Zhou, Y. Liu, H. Song, PRL 133, 192301 (2024); E. Nielsen (ALICE), A. Dattamunsi (CMS), QM2025;

III. Nuclear deformation and neutron skin in ^{96}Ru and ^{96}Zr nuclei

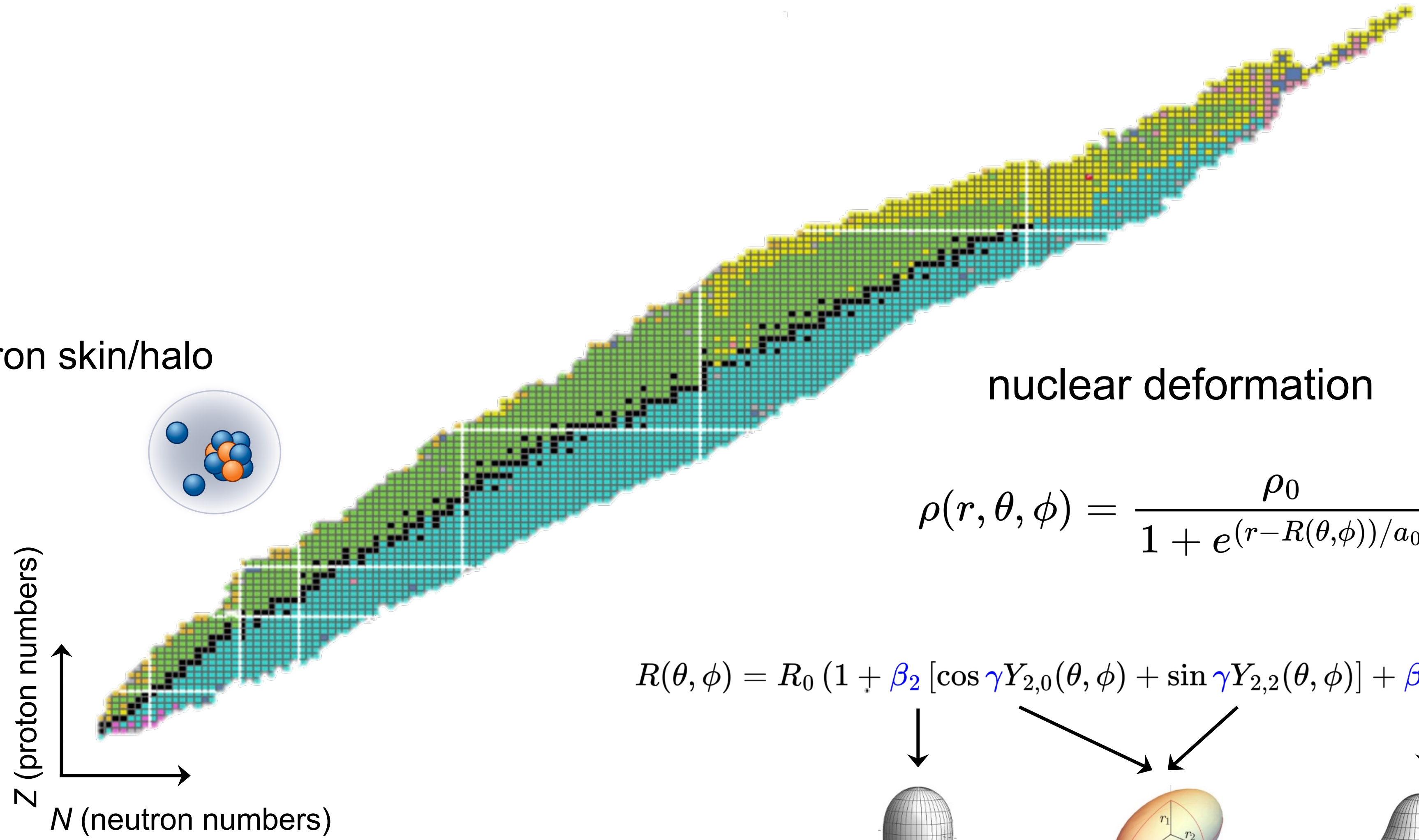

neutron skin/halo

nuclear deformation

$$\rho(r,\theta,\phi) = \frac{\rho_0}{1 + e^{(r - R(\theta,\phi))/a_0}}$$

$$R(\theta,\phi) = R_0\left(1 + \beta_2\left[\cos\gamma Y_{2,0}(\theta,\phi) + \sin\gamma Y_{2,2}(\theta,\phi)\right] + \beta_3 Y_{3,0}(\theta,\phi) + \beta_4 Y_{4,0}(\theta,\phi)\right)$$

Nuclear structure via collectivity v_n ratio

v_2 Ratio

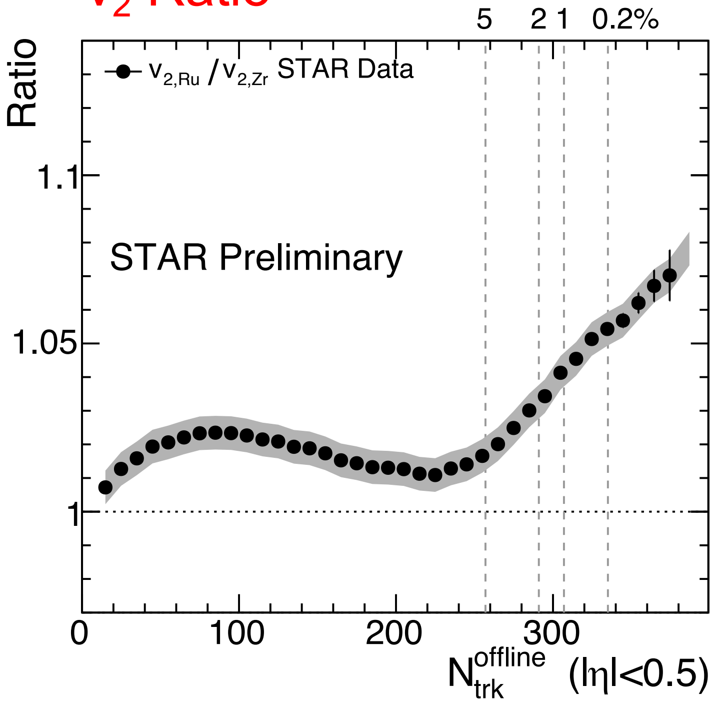

v_3 Ratio

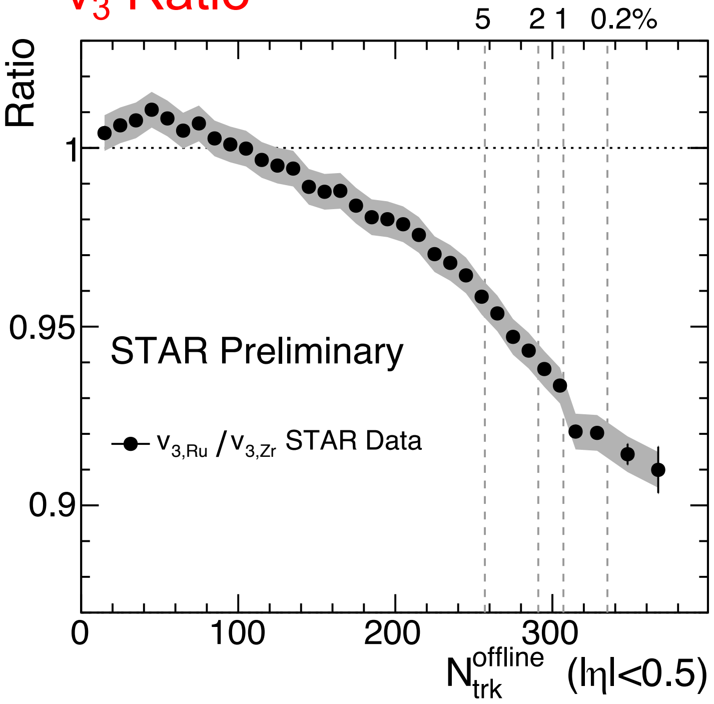

Nuclear structure via collectivity v_n ratio

v_2 Ratio

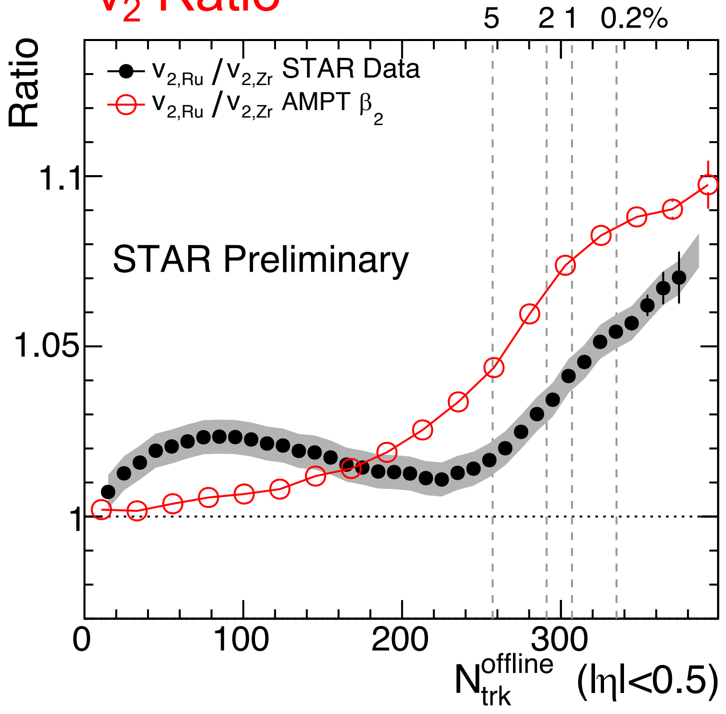

v_3 Ratio

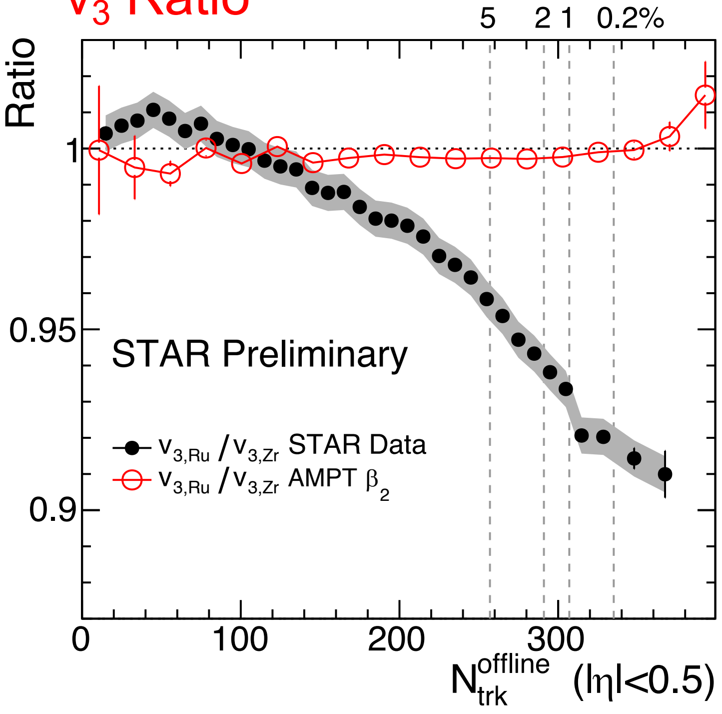

$\beta_{2,Ru}$ ~ 0.16 increase v_2, no influence on v_3 ratio

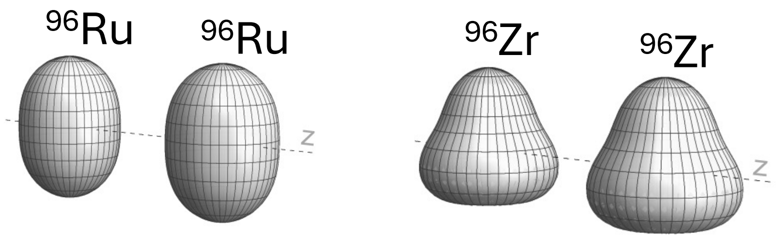

$$\beta_{2,\mathrm{Ru}} = 0.16 \pm 0.02$$

difference	$\Delta\beta_2^2$	$\Delta\beta_3^2$	Δa_0	ΔR_0
	0.0226	-0.04	-0.06 fm	0.07 fm

Current estimation is from transport model

C. Zhang and J. Jia, PRL128, 022301(2022); J. Jia, C. Zhang, PRC 107, L012901(2023)

Nuclear structure via collectivity v_n ratio

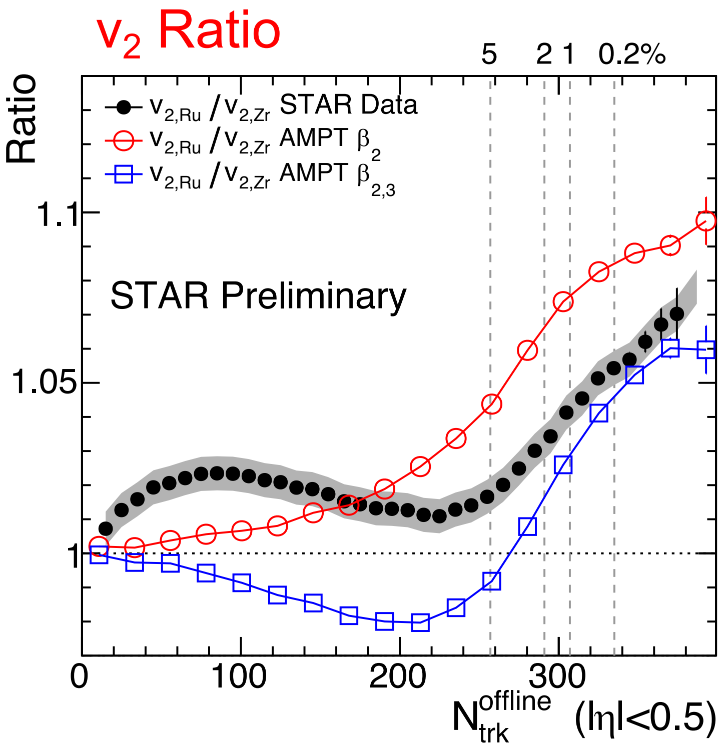

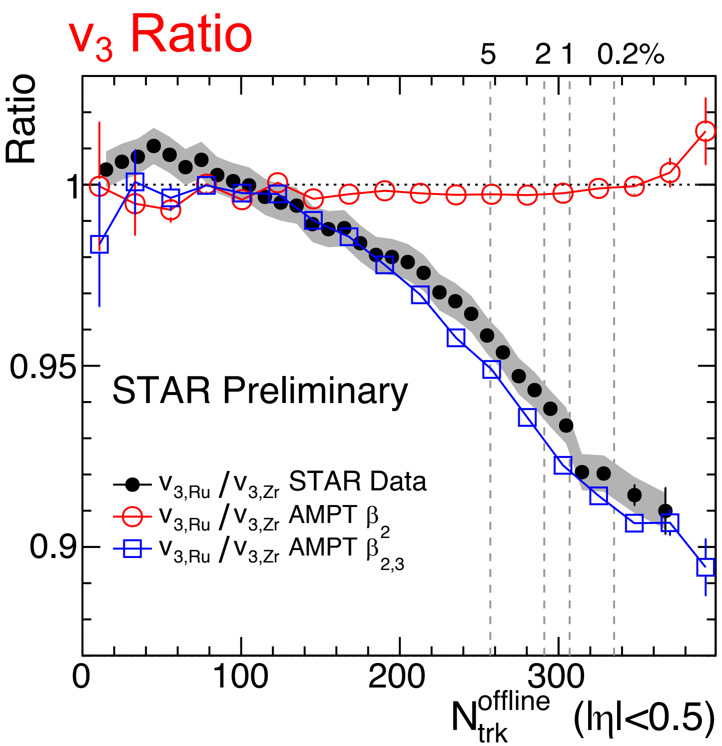

$\beta_{2,Ru}$ ~ 0.16 increase v_2, no influence on v_3 ratio

$\beta_{3,Zr}$ ~ 0.2 decrease v_2 in mid-central, decrease v_3 ratio

- Direct observation of octupole deformation in ^{96}Zr nucleus

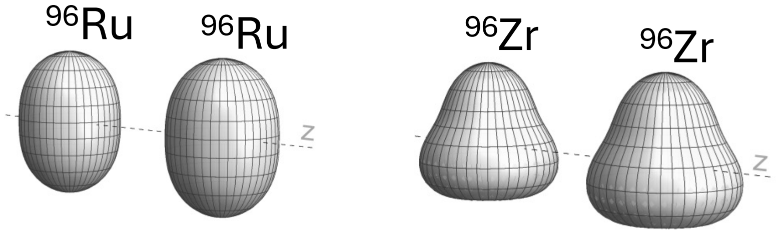

$\beta_{2,\mathrm{Ru}} = 0.16 \pm 0.02$ $\beta_{3,\mathrm{Zr}} = 0.20 \pm 0.02$

difference	$\Delta\beta_2^2$	$\Delta\beta_3^2$	Δa_0	ΔR_0
	0.0226	-0.04	-0.06 fm	0.07 fm

Current estimation is from transport model

C. Zhang and J. Jia, PRL128, 022301(2022); J. Jia, C. Zhang, PRC 107, L012901(2023)

Nuclear structure via collectivity v_n ratio

v_2 Ratio

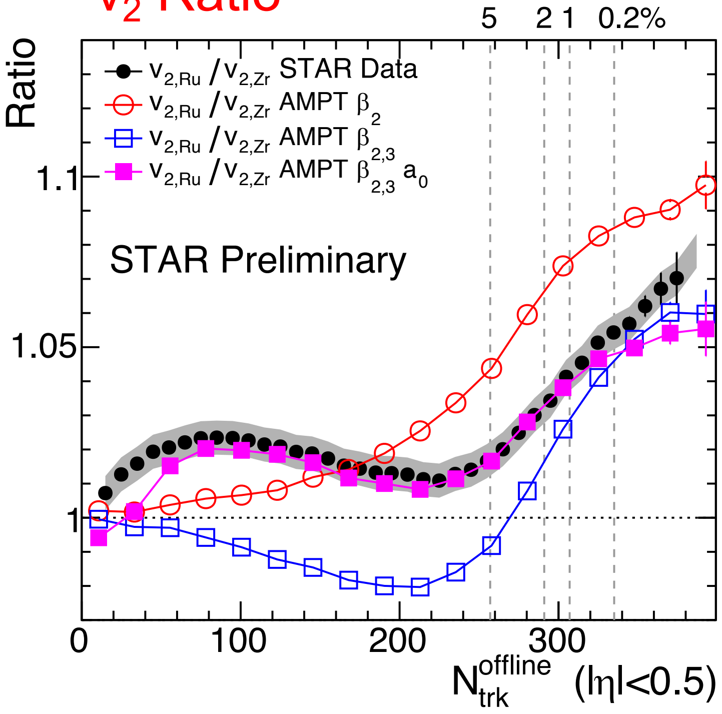

v_3 Ratio

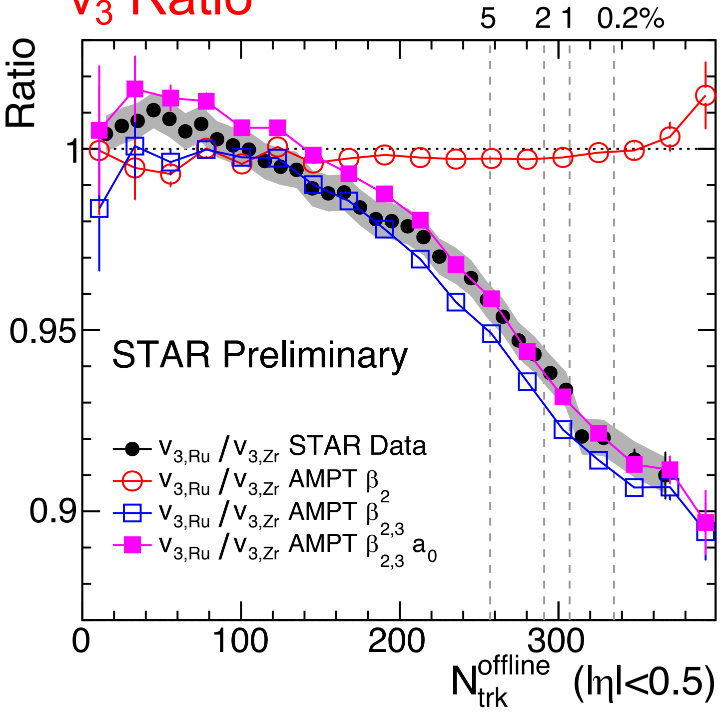

$\beta_{2,Ru} \sim 0.16$ increase v_2, no influence on v_3 ratio

$\beta_{3,Zr} \sim 0.2$ decrease v_2 in mid-central, decrease v_3 ratio

$\Delta a_0 = -0.06$ fm increase v_2 mid-central, small impact on v_3

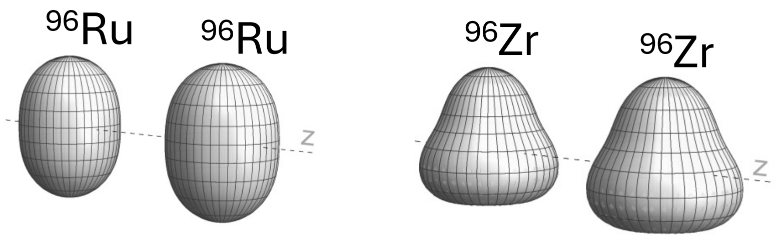

- Direct observation of octupole deformation in ^{96}Zr nucleus
- Imply the neutron skin difference between ^{96}Ru and ^{96}Zr

$\beta_{2,\mathrm{Ru}} = 0.16 \pm 0.02$ $\quad$ $\beta_{3,\mathrm{Zr}} = 0.20 \pm 0.02$

difference	$\Delta\beta_2^2$	$\Delta\beta_3^2$	Δa_0	ΔR_0
	0.0226	-0.04	-0.06 fm	0.07 fm

Current estimation is from transport model

C. Zhang and J. Jia, PRL128, 022301(2022); J. Jia, C. Zhang, PRC 107, L012901(2023)

Nuclear structure via collectivity v_n ratio

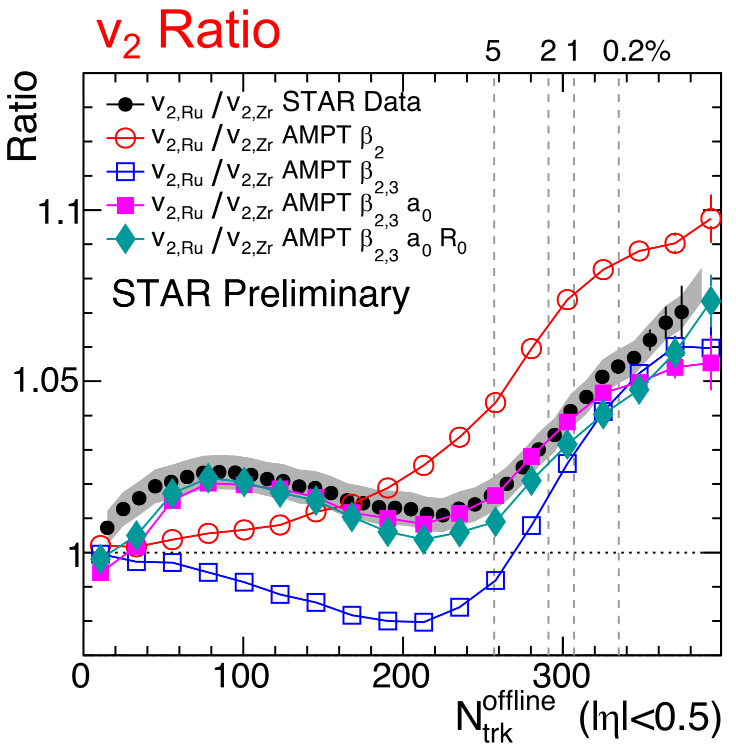

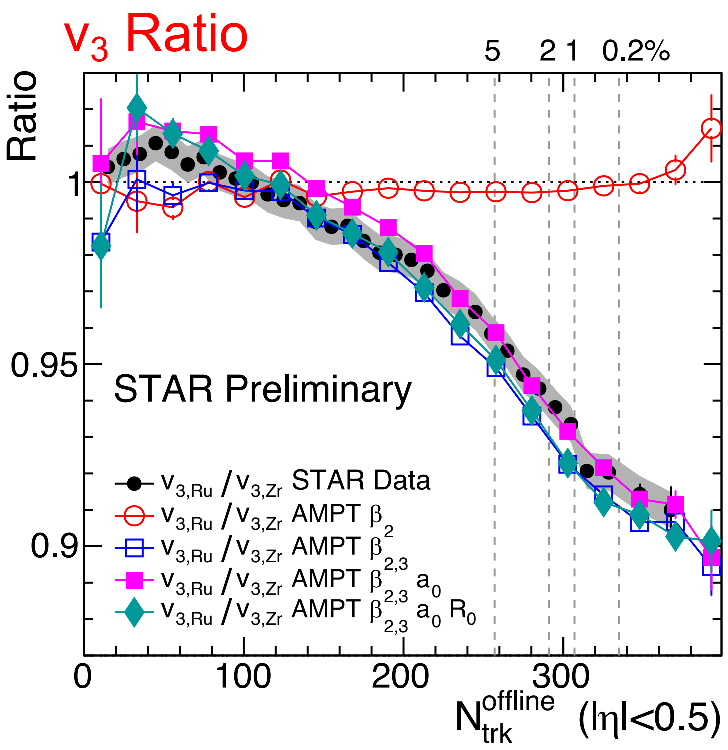

$\beta_{2,Ru}$ ~ 0.16 increase v_2, no influence on v_3 ratio

$\beta_{3,Zr}$ ~ 0.2 decrease v_2 in mid-central, decrease v_3 ratio

Δa_0 = -0.06 fm increase v_2 mid-central, small impact on v_3

Radius ΔR_0 = 0.07 fm only slightly affects v_2 and v_3 ratio.

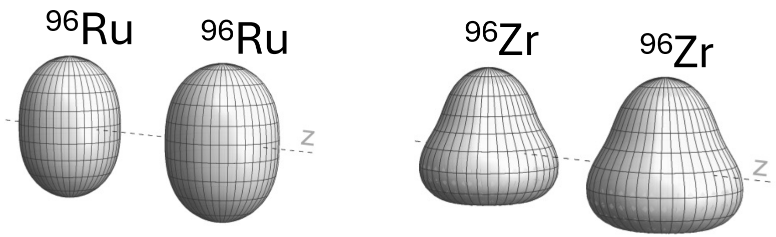

- Direct observation of octupole deformation in ^{96}Zr nucleus
- Imply the neutron skin difference between ^{96}Ru and ^{96}Zr
- Simultaneously constrain parameters using Bayesian analysis

$$R_{\mathcal{O}} \equiv \frac{\mathcal{O}_{\mathrm{Ru}}}{\mathcal{O}_{\mathrm{Zr}}} \approx 1 + c_1\Delta\beta_2^2 + c_2\Delta\beta_3^2 + c_3\Delta R_0 + c_4\Delta a$$

$\beta_{2,\mathrm{Ru}} = 0.16 \pm 0.02$ $\beta_{3,\mathrm{Zr}} = 0.20 \pm 0.02$

difference	$\Delta\beta_2^2$	$\Delta\beta_3^2$	Δa_0	ΔR_0
	0.0226	-0.04	-0.06 fm	0.07 fm

Current estimation is from transport model

C. Zhang and J. Jia, PRL128, 022301(2022); J. Jia, C. Zhang, PRC 107, L012901(2023)

Nuclear structure is inherent of heavy-ion probes

one-body distribution | two-body correlations | three-body correlations

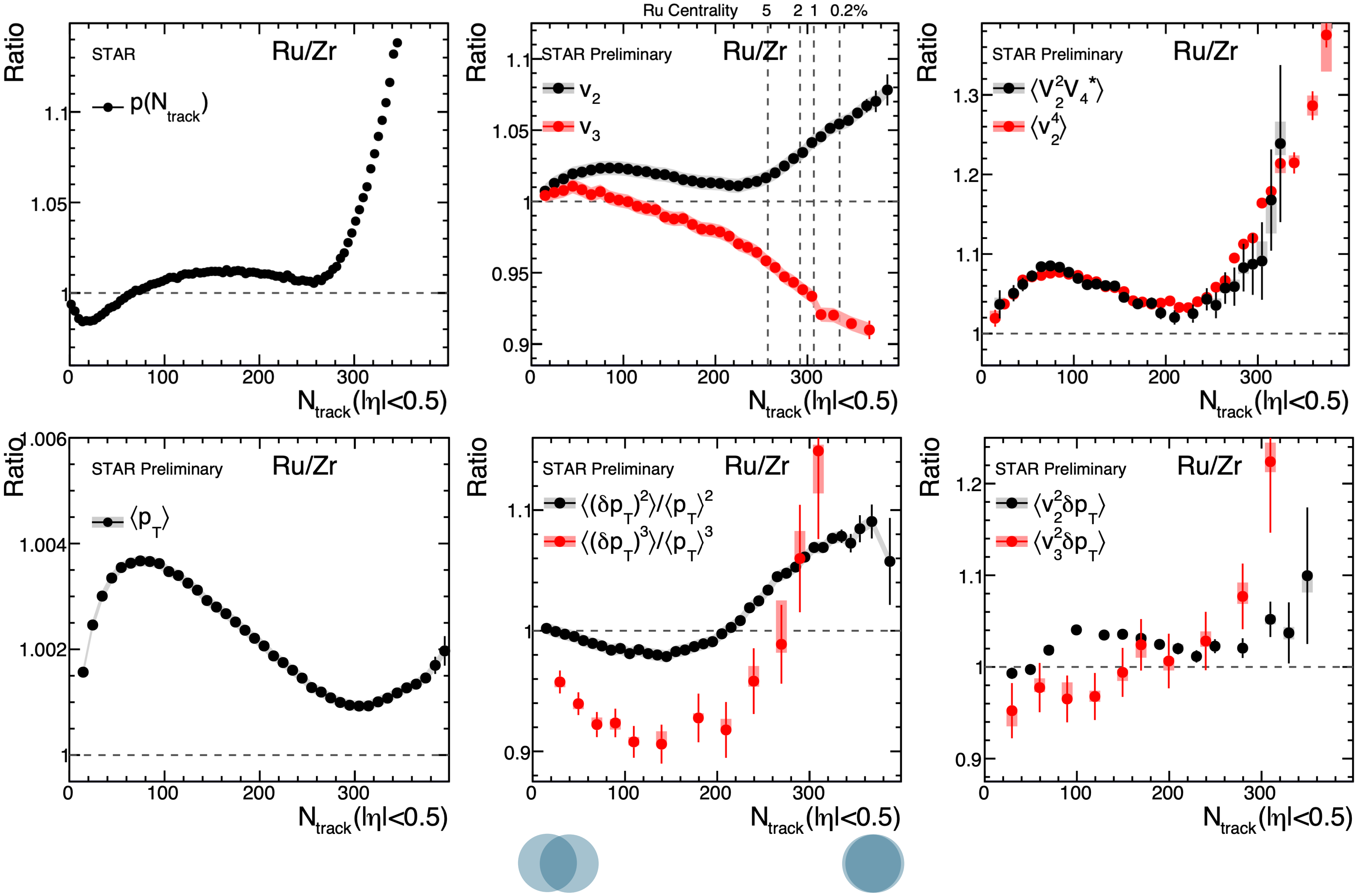

Imaging the radial structures (neutron skin)

Radial parameters R_0, a_0 are properties of one-body distribution → $\langle p_T \rangle$, $\langle N_{ch} \rangle$, $v_2^{RP} \sim v_2\{4\}$, σ_{tot},

H. Xu, QM2023

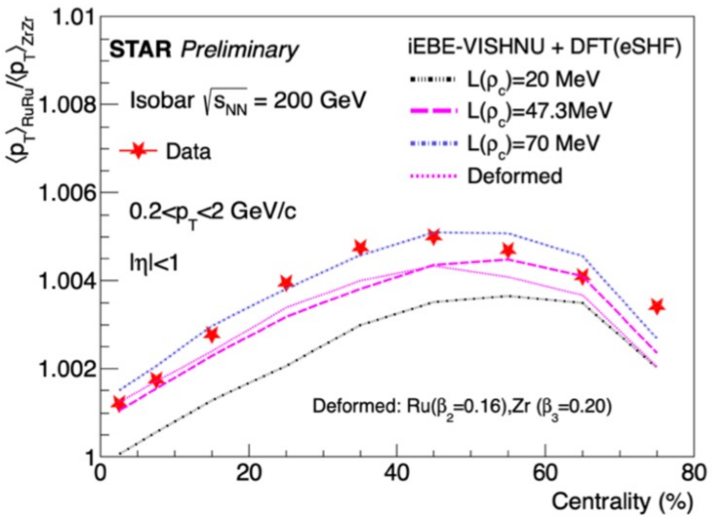

J. Jia, C. Zhang, PRC 107, L02901 (2023)

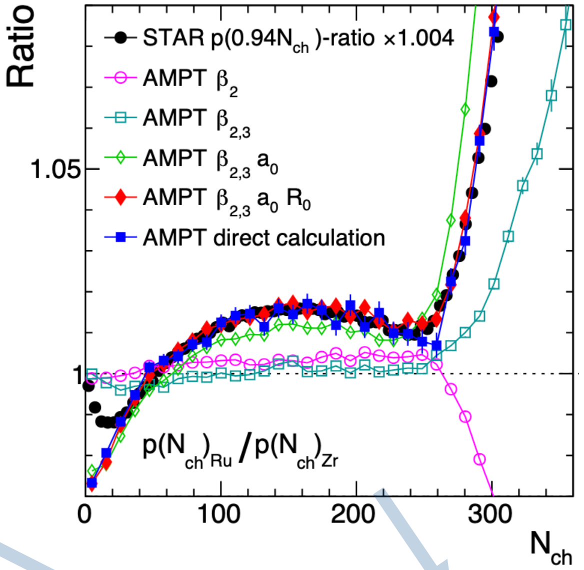

J. Jia, G. Giacalone, C. Zhang, PRL 131, 022301(2023)

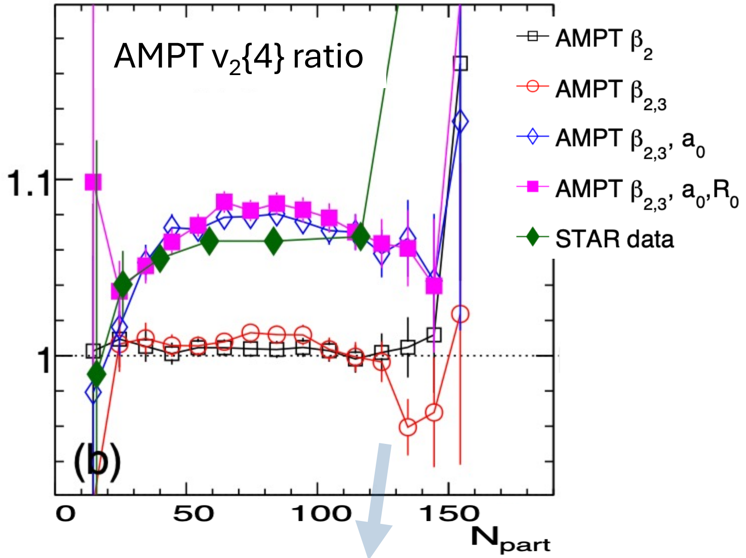

Current puzzle in low-energy nuclear physics

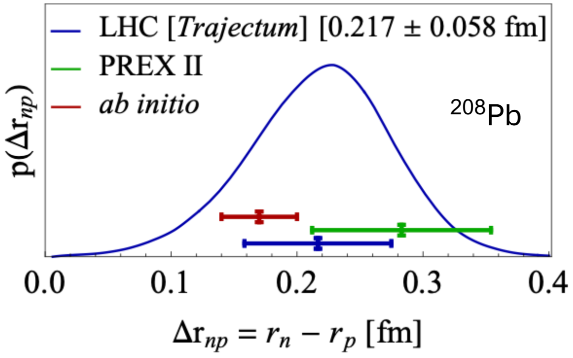

G. Giacalone, G. Nijs, W. Schee, PRL 131, 202302 (2023)

B. Li, et.al Universe 7, 182 (2021)

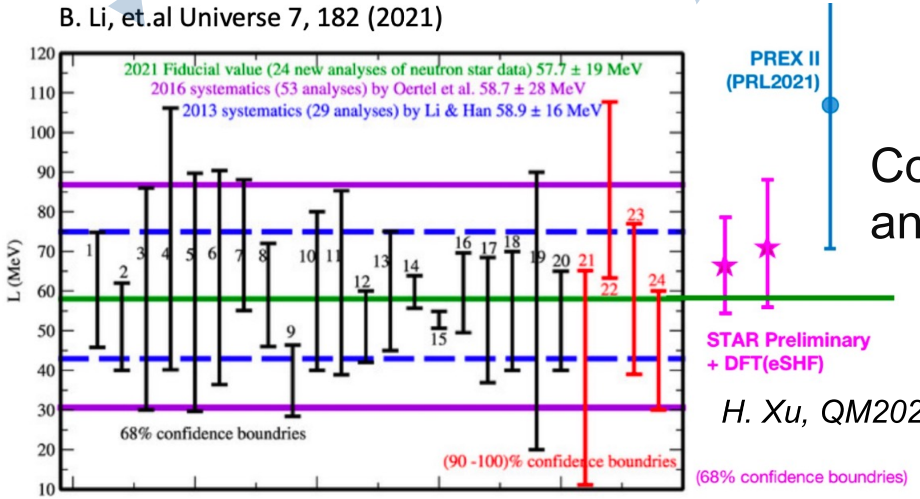

Constrain neutron skin and symmetry energy

H. Xu, QM2023

IV. Nucleonic clustering in ^{16}O nucleus

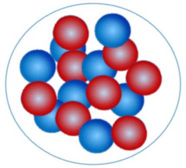

$$\rho(r) \propto \frac{1 + w(r^2/R^2)}{1 + e^{(r-R)/a_0}} \longrightarrow$$ first-principle ab initio framework

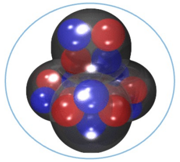

Hideki Yukawa

"for his prediction of the existence of mesons on the basis of theoretical work on nuclear forces"

nuclear cluster

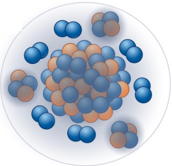

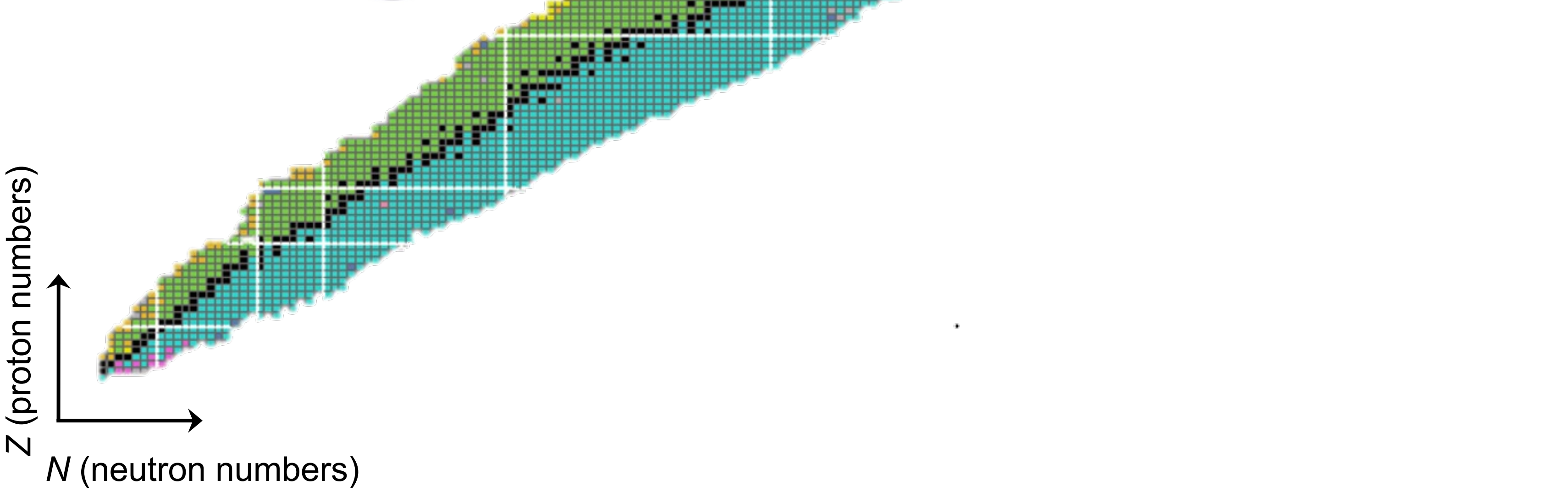

Nuclear geometry and nucleon nucleon correlations

Nucleon fluctuation

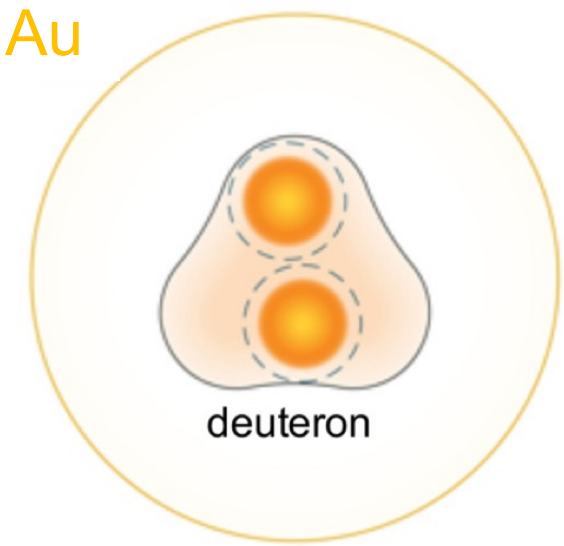

Nucleon & subnucleon fluctuation

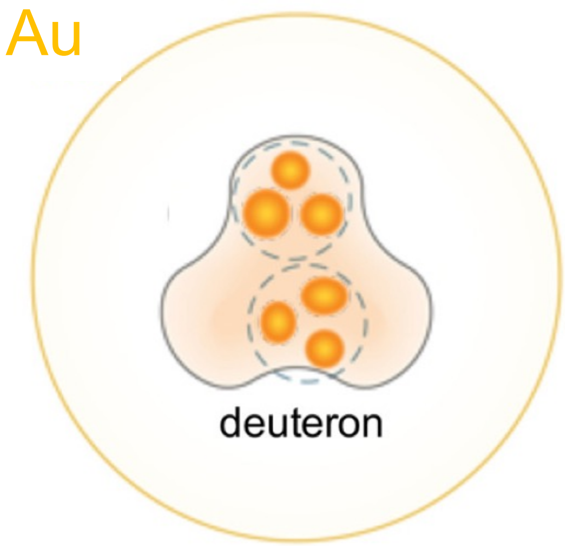

STAR, PRL 130, 242301 (2023)

STAR, PRC 110, 064902 (2024)

Nucleon-nucleon correlation

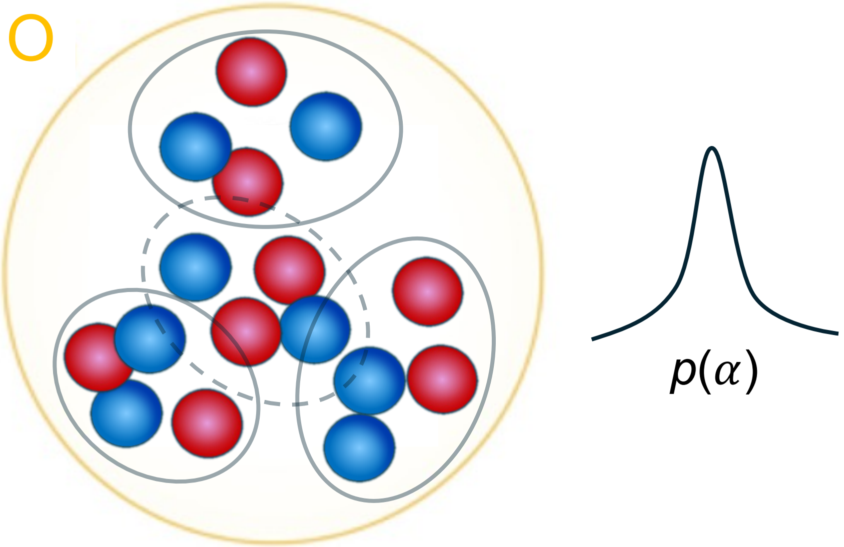

ab initio calculations

W. He, Y. Ma et al., PRL 113, 032506 (2014);…

C. Zhang, J. Chen, G. Giacalone, S. Huang, J. Jia, Y. Ma, PLB 862, 139322 (2025)

S. Huang, J. Jia, C. Zhang, 2507.16162

d+Au collision, 200 GeV ⟷ Nearly same N_{ch} ⟷ O+O collision, 200 GeV

Nucleon nucleon correlations in finite quantum many-body systems

Possible cluster in ground-state $^{16}_{8}O$ nuclei based on low energy, **low-energy experimental evidence?**

Woods-Saxon: ***without many-body nuclear correlation***

Nuclear Lattice Effective Field theory (NLEFT): model with many-nucleon correlation including α clusters

Lu et al., PLB797, 134863(2019)
M. Freer et al., RevModPhys90, 035004(2018)
S. Elhatisari et al. Nature 630, 59 (2024)

Variational auxiliary field diffusion Monte Carlo (VMC): *MC solution of Schrödinger eq. from the time evolution of trial wave function.*

A. Lonardoni et al., PRC97, 044318(2018)
J. Carlson and R. Schiavilla, RevModPhys70, 743(1998)

ab-initio Projected Generator Coordinate Method (PGCM): *Wave function from variational calculation (as in density functional theory*)

Frosini et al., EPJA58, 62(2022); EPJA58, 63(2022); EPJA58, 64(2022)

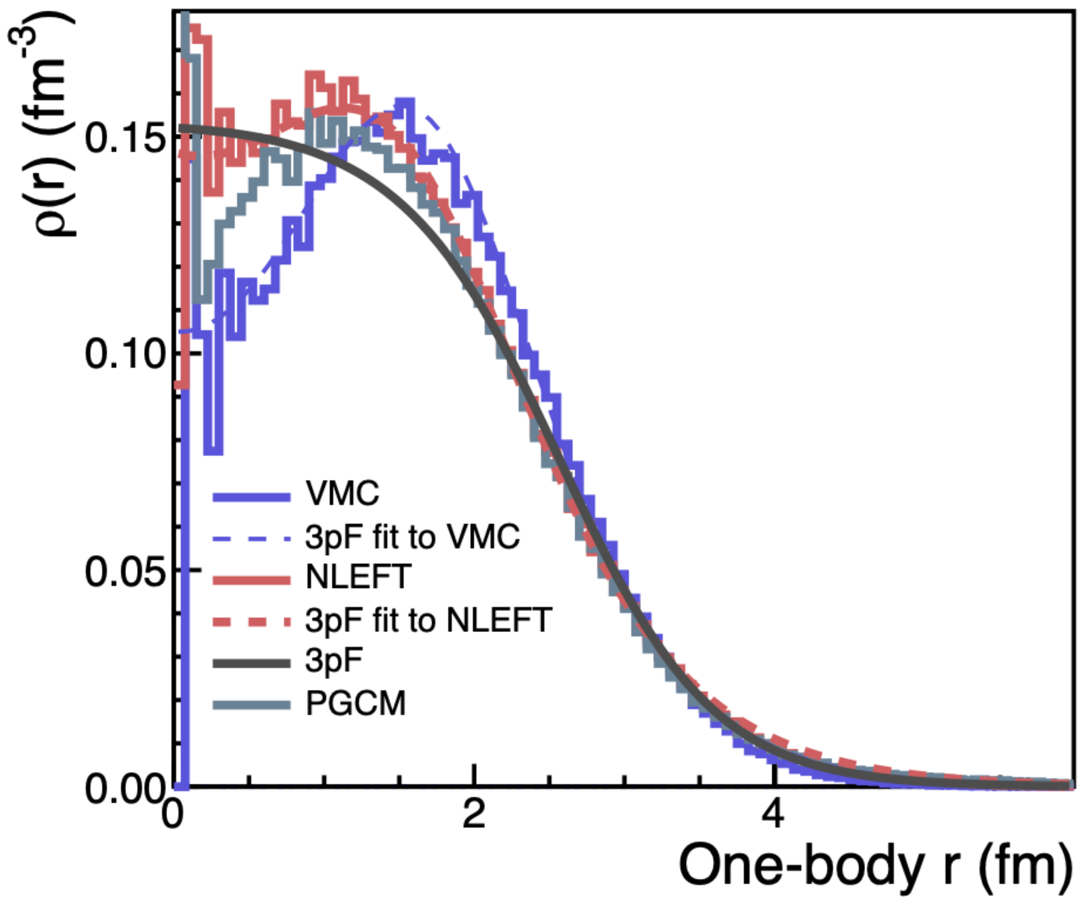

Benchmarking geometric tomography of ^{16}O nucleus

O+O run2021: 600M MB and 250M HM events

STAR manuscript is in preparation

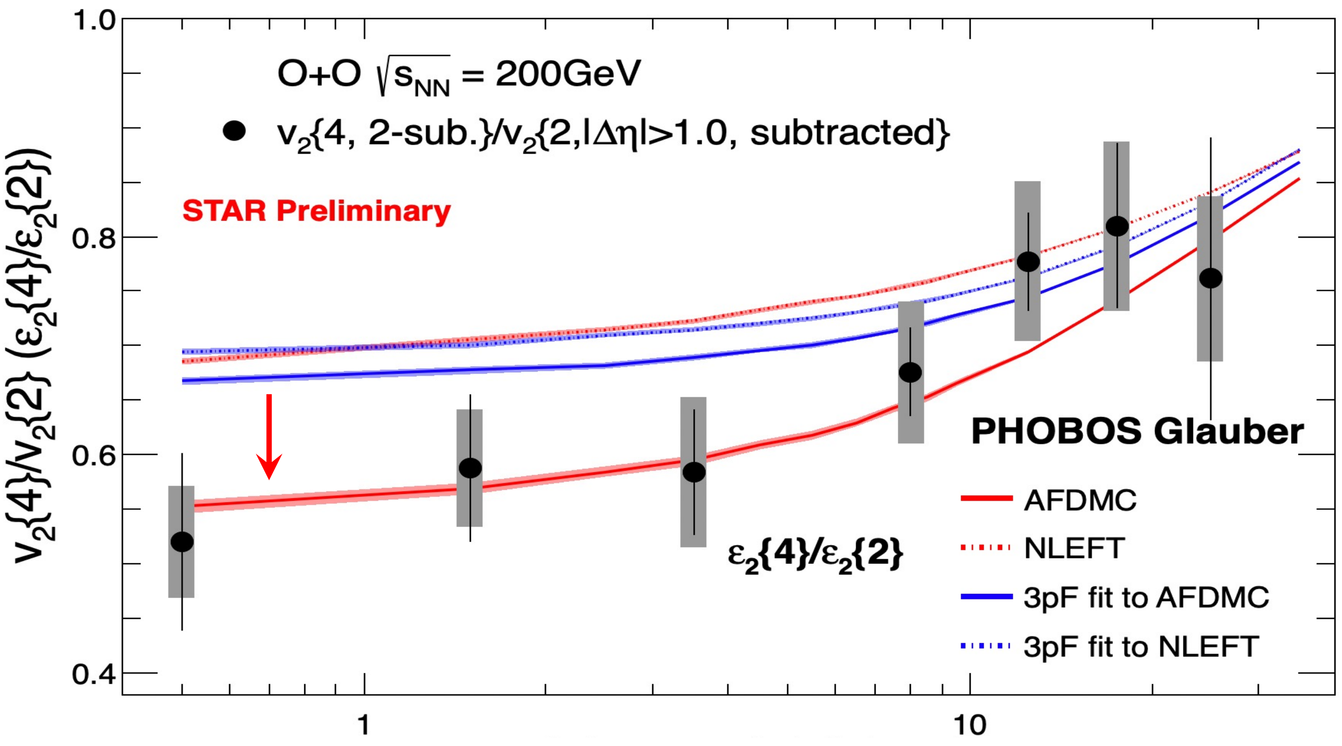

$$(v_n\{2\})^2 = c_n\{2\} = \langle v_n^2 \rangle \qquad \varepsilon_2\{2\}^2 = \langle \varepsilon_2^2 \rangle$$

$$(v_n\{4\})^4 = -c_n\{4\} = 2\langle v_n^2 \rangle^2 - \langle v_n^4 \rangle \qquad \varepsilon_2\{4\}^4 = 2\langle \varepsilon_2^2 \rangle^2 - \langle \varepsilon_2^4 \rangle$$

$\varepsilon_2\{4\}/\varepsilon_2\{2\}$ from three models:

1. WS is away from STAR data.

2. VMC and EFT have a visible difference.

Can many-nucleon correlations significantly impact the eccentricity fluctuations? YES!

VMC and EFT theory have visible differences describing the $v_2\{4\}/v_2\{2\}$. The interplay between sub-nucleon fluctuation and many-nucleon correlation.

STAR, PRL 130, 242301 (2023)

Y. Ma, S. Zhang, Handbook of Nuclear Physics (2022); W. He, Y. Ma et al, PRL 113, 032506 (2014)

C. Zhang, J. Chen, G. Giacalone, S. Huang, J. Jia, Y. Ma, PLB 862, 139322 (2025) G. Giacalone, G. Nijs et al., 2402.05995, G. Giacalone, W. Zhao et al., PRL134, 082301 (2025)

Y. Wang, S. Zhao, B. Cao, H. Xu and H. Song, PRC 109, L051904 (2024); X. Zhao, G. Ma. Y. Zhou, Z. Lin and C. Zhang, 2404.09780; S. Jahan, Roch, C. Shen, 2507. 11394

Benchmarking geometric tomography of ^{16}O nucleus

O+O run2021: 600M MB and 250M HM events; dAu: 70M MB

STAR manuscript is in preparation

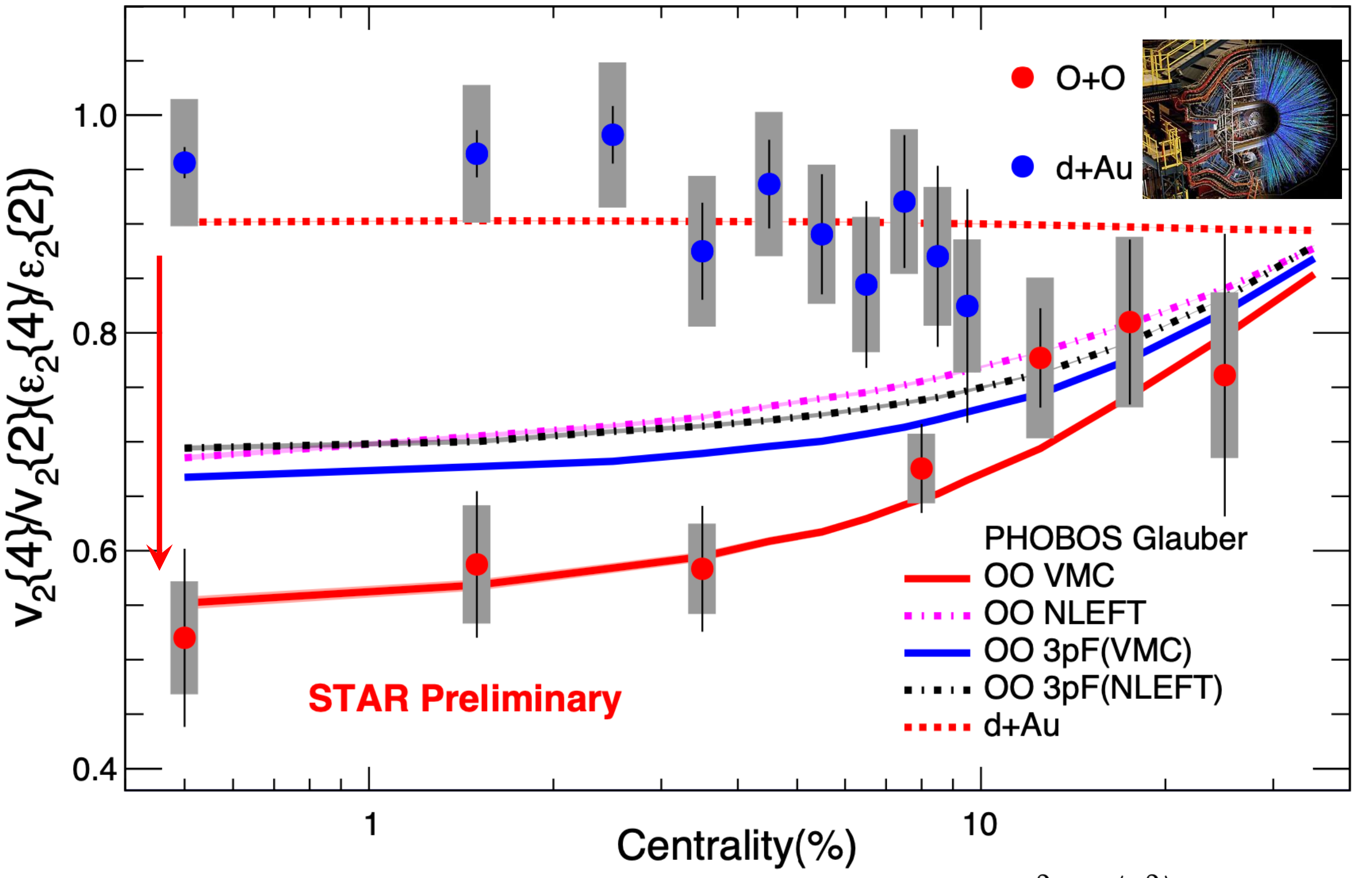

$$(v_n\{2\})^2 = c_n\{2\} = \langle v_n^2 \rangle$$
$$(v_n\{4\})^4 = -c_n\{4\} = 2\langle v_n^2 \rangle^2 - \langle v_n^4 \rangle$$

$$\varepsilon_2\{2\}^2 = \langle \varepsilon_2^2 \rangle$$
$$\varepsilon_2\{4\}^4 = 2\langle \varepsilon_2^2 \rangle^2 - \langle \varepsilon_2^4 \rangle$$

$\varepsilon_2\{4\}/\varepsilon_2\{2\}$ from three models:

1. WS is away from STAR data.

2. VMC and EFT have a visible difference.

Can many-nucleon correlations significantly impact the eccentricity fluctuations? YES!

VMC and EFT theory have visible differences describing the $v_2\{4\}/v_2\{2\}$. The interplay between sub-nucleon fluctuation and many-nucleon correlation.

STAR, PRL 130, 242301 (2023)

Geometric scan elucidates nuclear tomography and **strong nuclear force?**

Need more macroscopic model inputs.

p+O, O+O, and Ne+Ne at LHC Run2025

Y. Ma, S. Zhang, Handbook of Nuclear Physics (2022); W. He, Y. Ma et al, PRL 113, 032506 (2014)

C. Zhang, J. Chen, G. Giacalone, S. Huang, J. Jia, Y. Ma, PLB 862, 139322 (2025) G. Giacalone, G. Nijs et al., 2402.05995, G. Giacalone, W. Zhao et al., PRL134, 082301 (2025)

Y. Wang, S. Zhao, B. Cao, H. Xu and H. Song, PRC 109, L051904 (2024); X. Zhao, G. Ma. Y. Zhou, Z. Lin and C. Zhang, 2404.09780; S. Jahan, Roch, C. Shen, 2507. 11394

V. Conclusions and Outlooks

1. The signatures of nuclear structure in nuclear collisions are ubiquitous:

STAR, Nature 635, 67-72 (2024); 2506.17785

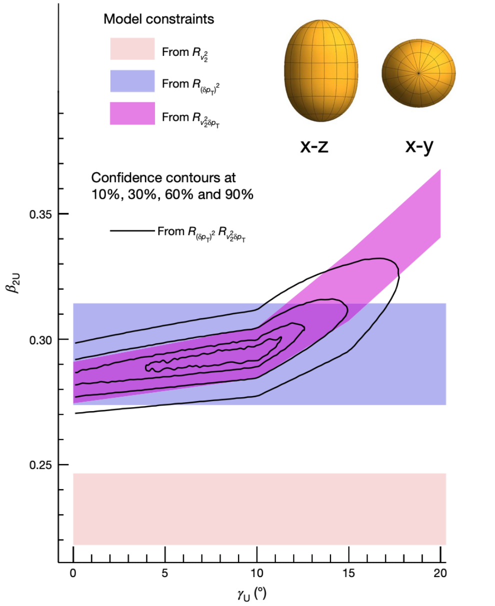

$\beta_{2U} = 0.286 \pm 0.025; \quad \gamma_U = 8.5^\circ \pm 4.8^\circ$

$\beta_{3U} = 0.08 - 0.1; \quad \beta_{3U} \sim \beta_{4U}$

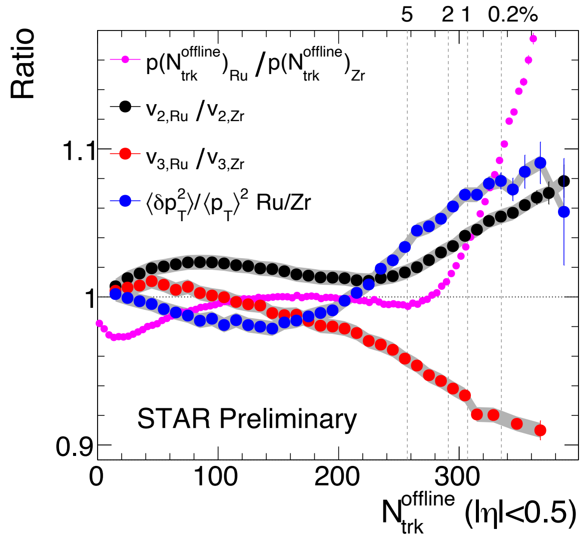

$\beta_{2,\mathrm{Ru}} = 0.16 \pm 0.02; \quad \beta_{3,\mathrm{Zr}} = 0.20 \pm 0.02$

difference	$\Delta\beta_2^2$	$\Delta\beta_3^2$	Δa_0	ΔR_0
	0.0226	-0.04	$-0.06\ fm$	$0.07\ fm$

STAR manuscript is in preparation

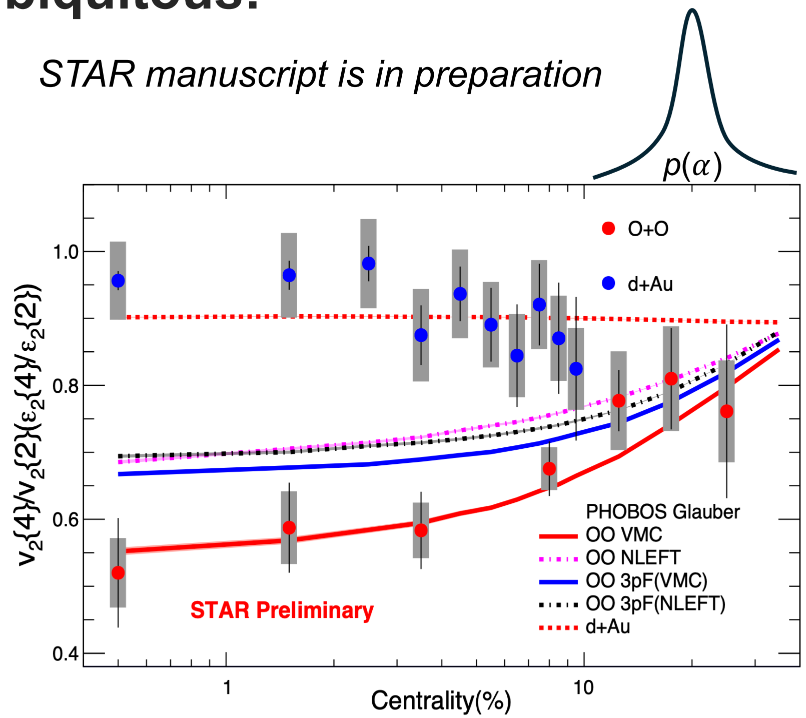

Nucleon-nucleon correlation is remarkable

Nuclear mass number (A)

2. Many potential applications from large to small collision systems :

→ Nucleosynthesis, nuclear fission, 0νββ

→ Rigid and soft β_n and γ (shape fluctuations/coexistence)

→ Neutron skin

→ Energy evolution between GeV/TeV and MeV in even-and odd-A nuclei

→ UPC- and AI-assisted nuclear shape imaging

Outline

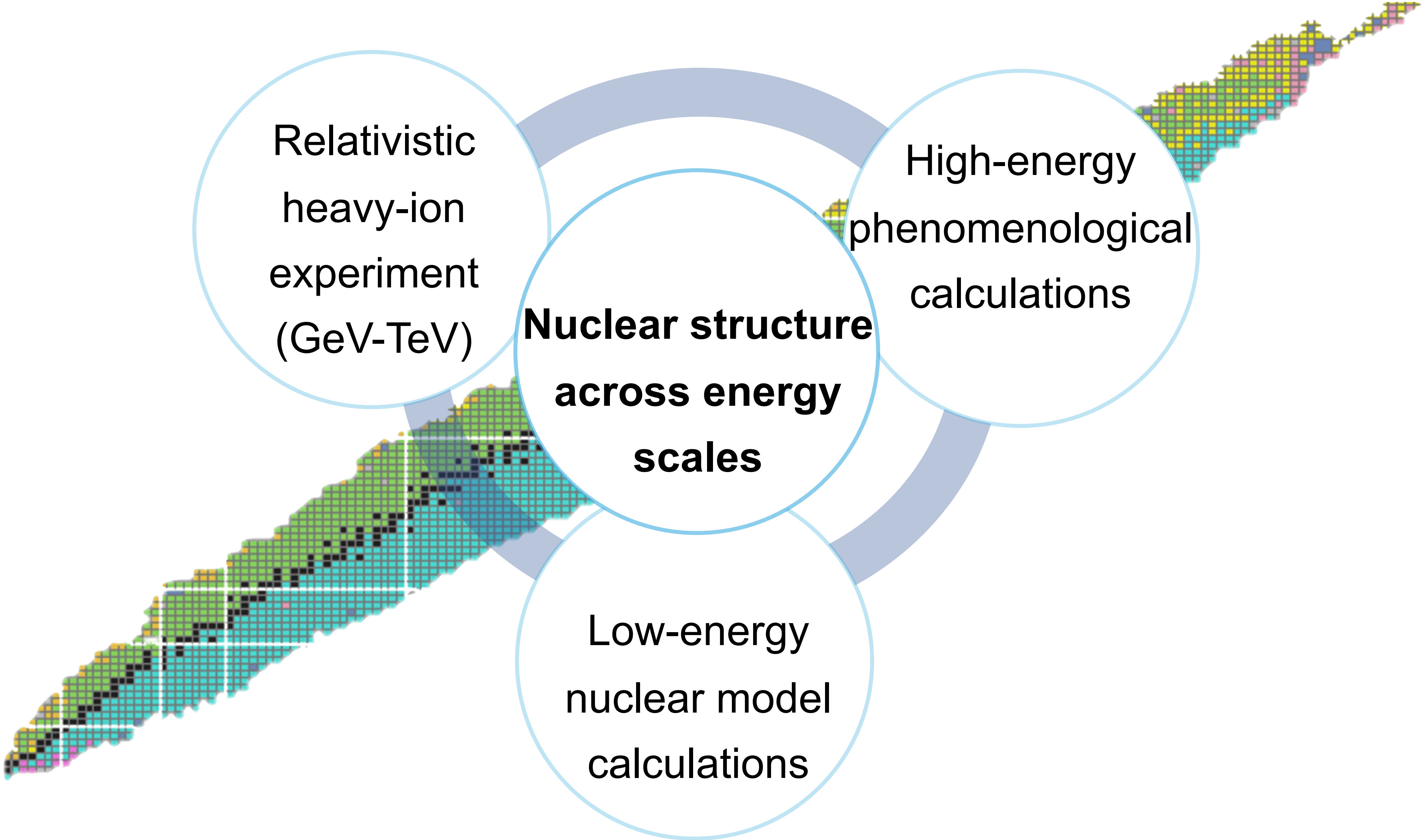
Relativistic heavy-ion experiment (GeV-TeV)
Nuclear structure across energy scales
High-energy phenomenological calculations
Low-energy nuclear model calculations

The past activities and nearest workshop

Recently organized activities from 2022:

RBRC workshop Jan 2022, link

EMMI Taskforce May&Oct 2022, link

ESNT workshop Sep 2022, link

INT program Jan-Feb 2023, link

Dalian workshop Aug 2023, link

Beijing workshop April 2024, link

CERN workshop Nov 2024, link

Intersection of nuclear structure and high-energy nuclear collisions: 2025 Program and Workshop, link

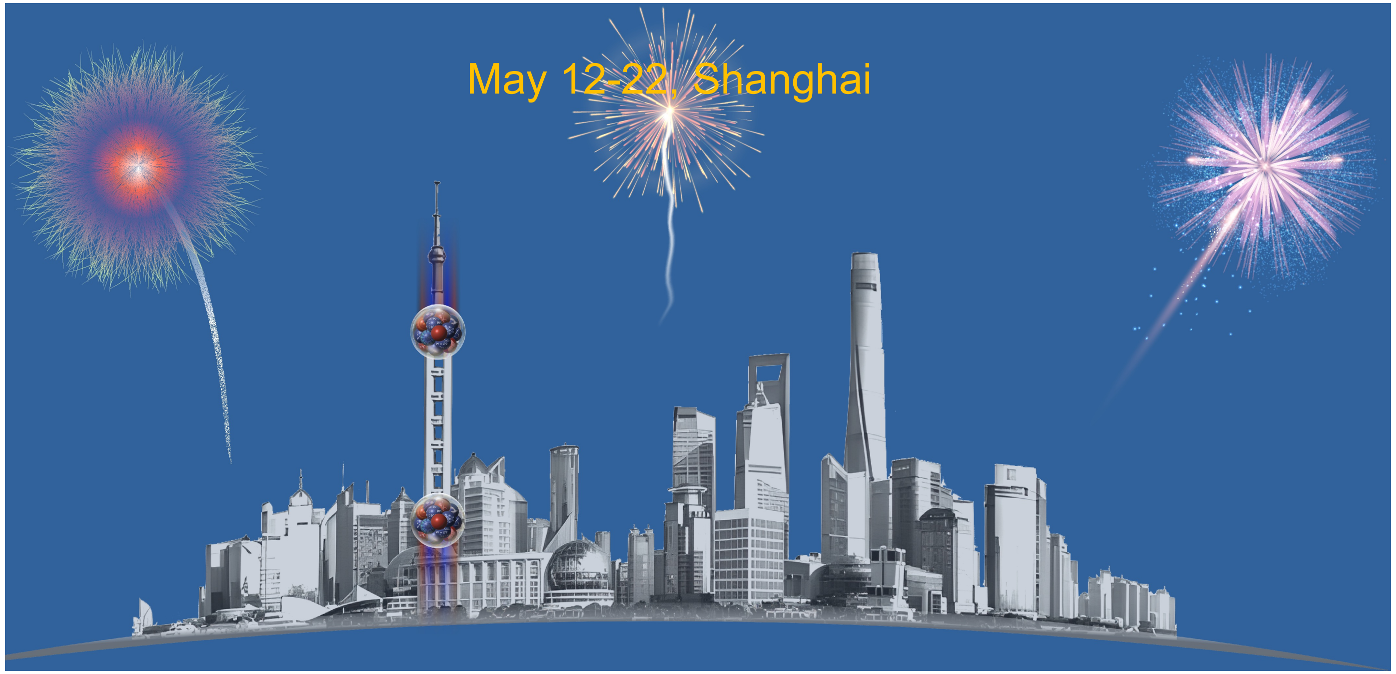

Nuclear structure in high-energy workshop in Sep. (Wuhan)

https://indico.ihep.ac.cn/event/25083/

Continue the efforts to further constrain QGP initial conditions and nuclear structure across energy scales.